TMRC-03-02

MDOT Research Report RC-1445

Causes and Cures for Cracking of Concrete Barriers

Final Report

Submitted to the

Michigan Department of Transportation

By

Thomas Van Dam, Ph.D., P.E.
Principal Investigator
Laetitia Delem
Karl R. Peterson
Larry L. Sutter, Ph.D.

Transportation Materials Research Center
Michigan Technological University
Dept. of Civil and Environmental Engineering
1400 Townsend Drive
Houghton, MI 49931

TESTING AND RESEARCH SECTION
CONSTRUCTION AND TECHNOLOGY DIVISION
RESEARCH REPORT NO. RC-1445

April 2004

TMRC-03-02

MDOT Research Report RC-1445

Causes and Cures for Cracking of Concrete Barriers

Final Report

Submitted to the

Michigan Department of Transportation

By

Thomas Van Dam, Ph.D., P.E.
Principal Investigator
Laetitia Delem
Karl R. Peterson
Larry L. Sutter, Ph.D.

Transportation Materials Research Center
Michigan Technological University
Dept. of Civil and Environmental Engineering
1400 Townsend Drive
Houghton, MI 49931

April 2004

New Abstract Form I:/forms/newblankabstractsheet (3/2002)

Technical Report Documentation Page

1. Report No. Research Report RC-1445	2. Government Accession No.	3. MDOT Project Manager John F. Staton
4. Title and Subtitle Causes and Cures for Cracking of Concrete Barriers		5. Report Date September, 2003
7. Author(s) Thomas J. Van Dam, Ph.D., P.E., Laetitia Delem, Karl R. Peterson, and Lawrence L. Sutter		6. Performing Organization Code
9. Performing Organization Name and Address Michigan Technological University 1400 Townsend Drive Houghton, MI 49931		8. Performing Org Report No. TMRC-03-02
12. Sponsoring Agency Name and Address Michigan Department of Transportation Construction and Technology Division P.O. Box 30049 Lansing, MI 48909		10. Work Unit No. (TRAIS) 11. Contract Number: 11(a). Authorization Number:
15. Supplementary Notes		13. Type of Report & Period Covered Final 14. Sponsoring Agency Code

16. Abstract

In recent years, greater numbers of prematurely deteriorated concrete barriers have been observed in Michigan. The main forms of distress observed are map cracking, vertical transverse cracking, horizontal cracking, delamination, pop-outs, scaling, and disintegration. This report presents the results of a microsctructural evaluation of concrete from eight bridge locations. The analysis included visual assessment and a full petrographic evaluation, which included stereo and petrographic optical microscopy, x-ray analytical microscopy, and scanning electron microscopy. Also, the parameters of the air-void system were determined in accordance with ASTM C457, and a staining method was used for the measurement of carbonation depth. In all cases, the concrete was observed to have greater than normal levels of entrapped air, which in some cases was severe. It was also found that the concrete from one-third of the locations has air-void system parameters that were marginal to deficient in their ability to protect the concrete against damage from cyclic freezing and thawing. A contributing factor in this observation was the infilling of the air-void systems with secondary ettringite. It was also observed that certain chert and siltstone constituents of the fine aggregate were alkali-silica reactive in the presence of slag coarse aggregate. Based on these findings, it is recommended that better consolidation techniques be employed in the construction of concrete barriers, that freeze-thaw durability cannot be ensured simply by measuring the total air volume, but instead the air-void system parameters must be assessed, and that the occurrence of alkali-silica reactivity of chert and siltstone constituents of the fine aggregate in the presence of slag coarse aggregate must be studied.

17. Key Words concrete durability, materials-related distress, alkali-silica reactivity, bridge barriers	18. Distribution Statement No restrictions. This document is available to the public through the Michigan Department of Transportation.		
19. Security Classification (report) Unclassified	20. Security Classification (Page) Unclassified	21. No of Pages 61	22. Price

Table of Contents

List of Figures

List of Tables

Executive Summary

Background

In recent years, greater numbers of prematurely deteriorated concrete barriers have been observed in Michigan. The main forms of distress observed are map cracking, vertical transverse cracking, horizontal cracking, delamination, pop-outs, scaling, and disintegration. Possible factors contributing to the early deterioration of the current generation of barriers used by the Michigan Department of Transportation (MDOT) are the changes in design features, construction practices related to casting/consolidation of the concretes, curing, and type of materials used.

The work presented in this study was part of a joint research effort between Wayne State University (WSU) and Michigan Technological University (Michigan Tech) through the Center for Structural Durability. The overall project, funded by MDOT, was conducted to identify the root cause of the observed deterioration of concrete barriers in Michigan and to make recommendations to alleviate such deterioration in future barriers. WSU was responsible for the inspection of existing barriers and the monitoring of new constructions, for non- destructive and permeability testing, and for sampling of existing barriers. The work conducted at Michigan Tech and presented in this report focused on the microstructural examination of concrete extracted from barriers in order to assess the types of materials-related distresses present in Michigan's concrete bridge barriers.

In order to identify possible factors contributing to the early deterioration of the current generation of barriers used by MDOT, sixteen cores extracted from bridge barriers from eight different locations in Michigan were inspected according to the procedures presented in the FHWA guidelines (Van Dam 2002b).

The samples were subjected to a full petrographic evaluation, which included stereo and petrographic optical microscopy, x-ray analytical microscopy, and scanning electron microscopy. Also, the parameters of the air-void system were determined in accordance with ASTM C457, and a staining method was used for the measurement of carbonation depth.

Key Findings

Based on visual and stereo-optical inspection, all observed cores showed some kind of consolidation problems. Entrapped air voids from varying sizes were common around aggregates and the steel reinforcement. No grossly low existing air contents were measured (using ASTM C457); however, one third of the samples had spacing factors that are considered marginal for protecting the paste from freeze-thaw damage. These high spacing factors were attributed to a lack of entrained air voids, an extensive amount of infilling, or a combination of the two.

In stereo and petrographic optical examination, alkali-silica reactivity was observed in the fine aggregate fraction of the two test sites containing blast furnace slag coarse aggregates. The reactivity of the cherts and siltstones particles in the fine aggregate was confirmed by x-ray microscopy. Similar siltstones were observed in concrete from another site that did not contain slag coarse aggregate; however, in that case the siltstones was not observed to be reactive and the limited damage was attributed to freezing and thawing. The frost-susceptibility of the siltstones, as well as the presence of secondary ettringite in air voids, might also have exacerbated the distress caused by ASR in locations where slag coarse aggregate was used.

Finally, significant steel corrosion was observed in only one location. In that case the corrosion was so severe that it had led to delamination of the concrete. The carbonation depths measured from samples obtained at this location were also higher than normal, which indicates that the corrosion might result from a higher permeability to water and aggressive agents (deicer salts).

Recommendations

Based on these observations, it is recommended that better consolidation of the concrete barriers be required, as this will minimize the ubiquitous entrapped air that was observed at all locations. This entrapped air reduces the strength of the concrete as well as providing ready pathways for the ingress of water and aggressive chemical agents (e.g. deicers), reducing the life of the barriers.

It is also recommended the air-void system parameters be verified for the specific job mix formula being used. It is well known that the ability of a given air entraining agent to created an adequate air-void system is affected by the cement and other admixtures used, and that the control of air volume alone is

not sufficient to ensure freeze-thaw durability. A more rigorous approach to the assessment of the air-void system parameters of the concrete would significantly enhance the freeze-thaw durability of these concrete barriers.

It is recommended that a study be initiated to evaluate the nature of the relationship between alkali-silica reactivity (ASR) in the chert and siltstones constituents of the fine aggregates and the presence of slag coarse aggregate in the concrete. ASR was only observed at those locations where slag coarse aggregate was used. This study would need to consider a broad range of factors including, but not limited to, the alkali content of the cement, the impact of supplementary cementitious materials, and the type and volume of reactive constituents in the fine aggregate.

Deposits of ettringite were commonly observed in the air voids of several of the cores evaluated in this study. It would therefore be useful to determine the sulfate content of the samples to evaluate if there is any relationship between sulfate content and amount of infilling. The determination of the sulfate content would be particularly interesting in the case of the concrete with slag coarse aggregate, because, based on previous research conducted at Michigan Tech, the dissolution of calcium sulfide from blast furnace slag aggregates may provide an internal source of sulfate possibly promoting the formation of ettringite (Peterson 1999, Hammerling 1999, Hammerling 2000).

Finally, tests should be conducted to evaluate the frost-susceptibility of the deteriorated fine siltstones observed at some locations to determine its contribution, if any, to the observed deterioration.

Chapter 1. Introduction

In recent years, greater numbers of prematurely deteriorated concrete barriers have been observed in Michigan. The main forms of distress observed are map cracking, vertical transverse cracking, horizontal cracking, delamination, pop-outs, scaling, and disintegration. Possible factors contributing to the early deterioration of the current generation of barriers used by the Michigan Department of Transportation (MDOT) are the changes in design features, construction practices related to casting/consolidation of the concretes, curing, and type of materials used.

The work presented in this final report was part of a joint research effort between Wayne State University (WSU) and Michigan Technological University (Michigan Tech) through the Center for Structural Durability. The overall project, funded by MDOT, was conducted to identify the root cause of the observed deterioration of concrete barriers in Michigan and to make recommendations to alleviate such deterioration in future barriers. WSU was responsible for the inspection of existing barriers and the monitoring of new constructions, for non- destructive and permeability testing, and for sampling of existing barriers. The work conducted at Michigan Tech and presented in this report focused on the microstructural examination of concrete extracted from barriers in order to assess the types of materials-related distresses present in Michigan's concrete bridge barriers.

In total, sixteen cores of concrete bridge barriers from eight different locations in Michigan, constructed between 1983 and 2001 were provided to Michigan Tech by WSU. These samples were inspected according to the techniques detailed in the FHWA report entitled, "Guidelines for Detection, Analysis, and Treatment of Materials-Related Distress in Concrete Pavements – Volume 2."(Van Dam 2002b). A petrographic evaluation was performed which included stereo and petrographic optical microscopy, x-ray analytical microscopy, and scanning electron microscopy equipped with an energy dispersive spectrometer. The air-void system parameters were quantified in accordance with ASTM C457, and other measurements were made to characterize the depth of carbonation. From this analysis, a thorough understanding of the microstructural features leading to distress in concrete barriers was formulated.

The need for this research effort was established in a report prepared by J.F. Staton and J. Knauff (1999), entitled *Evaluation of Michigan's Concrete Barriers*. The observations made in the report indicated that many of the current generation barriers used by MDOT are deteriorating at a rate greater than expected. According to the report, prior to 1960's, standard bridge railings were Type R-4 and R-5. From 1961 through the 1970's barrier Types R-11 and R-12 were constructed. Also, in 1967 a barrier design named G.M. (Type 1) was adopted with a height of 32 in and a truncated trapezoidal cross section of 16 in at the base and 6 in at the top. In 1976, the New Jersey (Type 2) and in 1977, the New Jersey (Type 3) were adopted. In 1982, the cross-section of the Type 2 and 3 was modified and new standard design configurations (Types 4 and 5) were developed.

The common construction practice of "slip-form" casting of concrete barriers appears to have started in 1972. In this casting practice, a very low slump concrete is placed as the form is pulled, generating an extruded concrete barrier profile. Little or no external vibrating is performed in order to retain the extruded barrier shape.

This report is comprised of five chapters. Chapter 2 provides the background, based on the available literature, needed to understand the durability issues surrounding concrete barriers. Chapter 3 presents the experimental procedures, followed by results and discussion in Chapter 4. The conclusions and recommendations based on this study are presented in Chapter 5. Appendices are used to present the data in project portfolio format.

Chapter 2. Background

The failure of a concrete structure can be associated with inadequate structural design and/or improper construction, and also with the properties of the materials used and their interaction with the environment in which the structure is placed. Materials-related distresses (MRD) mostly affect the long-term performance (durability) of the concrete and are generally manifest as fine cracking or material degradation that can progress to complete deterioration of the structure. Their occurrence is mainly dependent on the constituent materials, the climatic conditions, and the presence of external aggressive agents (e.g. roadway deicing chemicals).

A distinction is often made between types of MRD that are caused by physical mechanisms versus chemical mechanisms, although the distress is most often the result of an interaction of both. Also, it is not uncommon that different types of MRD are present in one structure, because the distress caused by one type often initiates or aggravates another type. It is therefore often difficult to determine the primary cause of distress.

Physical mechanisms that could affect concrete barriers in Michigan include freeze-thaw deterioration of hardened cement paste and aggregates, and deicer scaling attack. Alkali-silica reactivity (ASR), alkali-carbonate reaction (ACR), sulfate attack, and corrosion of embedded steel are types of MRD that originate from a chemical mechanism. A detailed overview of the most common types of MRD is given in "Guidelines for Detection, Analysis, and Treatment of Materials-Related Distress in Concrete Pavements – Volume 1 (Van Dam 2002a)."

Only deterioration due to freezing and thawing and ASR is discussed in detail in the present chapter because these were the main types of MRD observed in the course of this study. A brief section is also devoted to ettringite and its occurrence in mature concrete, as it was observed infilling the air voids of many samples. Finally, the last section of this chapter discusses carbonation, because although it is not in itself a type of MRD, its presence contributes to the corrosion of embedded steel in reinforced concrete. Moreover, the carbonation depth reflects the permeability of the outer layers of concrete and can thus be used to assess the quality of the concrete.

2.1 Durability of Concrete Subjected to Freezing and Thawing

Frost action and exposure to deicing salts are important causes of deterioration of concrete transportation structures in cold climates. An adequate air-void system is the most common way to increase the resistance of concrete to repeated freezing and thawing cycles, but many other factors have an influence on the frost resistance of concrete. This section provides an overview of the existing theories of frost action and deicer salt scaling mechanisms. It also portrays the role and the characteristics of an efficient entrained air-void system, its production, and how to compute its parameters in hardened concrete. Finally, it presents some other factors, like the materials and mix characteristics, affecting the frost resistance of concrete.

2.1.1 Theories of frost action and deicer salt scaling mechanisms

2.1.1.1 Theories of frost action

During the hydration process, portland cement and water react to form hardened paste that binds together the coarse and fine aggregates. In normally proportioned concrete, the hydration products will never fill all the water-filled space that existed between the cement grains, the result being that some voids will remain. These voids, known as capillary pores, vary in size from 5nm to 1μm[1]. In the worst case, they can form an interconnected network through which bulk water can flow and ionic diffusion can occur relatively easily (St. John 1998, Pigeon 1995, Mindess 2003).

The degree of saturation of these pores will depend on the relative humidity of the atmosphere surrounding the concrete, whether the concrete is in contact with a source of water (like the ground), and the size of the pores. A number of theories exist to explain the damage that is incurred by concrete subject to freezing and thawing in a saturated or near-saturated state; the three most important are presented in the following paragraphs.

The oldest and most well known frost action theory is the hydraulic pressure theory developed by Powers in 1949. Powers postulated that if the temperature decreases well below 32 °F in

[1] Note: This report uses English units except when reporting microstructural measurements which are reported in SI units. This follows standard industrial convention for such meausurements.

saturated cement paste, ice will begin to form in the capillary pores (the freezing point of water in capillary pores is well below 32 °F because of the surface tension and the presence of ionic species). The 9 percent increase in volume associated with ice formation will force water out of the capillaries, generating tensile stresses in the paste. The pressure developed in the matrix increases with the rate of cooling, the rate of ice formation, and the maximum distance that water must travel to reach an escape boundary, but decreases as the hydrated cement paste permeability increases. Cracking occurs when the pressure generated by the flow is greater than the tensile strength of the paste (Pigeon 1995).

This theory has been considered invalid by most contemporary researchers, including Powers himself, because it cannot account for all the phenomena observed as concrete freezes. For instance, it cannot explain why porous materials can be damaged by freezing and thawing when they are saturated with organic liquids that do not expand upon freezing (Marchand 1994, Pigeon 1995, Mindess 2003).

In the beginning of the 1950's, Powers observed in his subsequent investigations that after an initial expansion, air-entrained pastes tend to contract upon freezing. This led him to the conclusion that during freezing the water tends to move to and not from the capillary pores where ice is forming. This formed the basis for his osmotic pressure theory. The fluid contained in capillary pores is not pure water, but an ionic solution that is in equilibrium with the hydrated paste. Consequently, when water in the larger pores turns to ice, not all of the water will freeze due to the dissolved ions present.

As ice forms, the concentration of dissolved chemicals in the remaining water increases, becoming higher than the concentration of the liquid water contained in the surrounding smaller pores. That difference in concentration drives water from the smaller pores to the larger pores by osmosis. The osmotic pressure due to the movement of water can cause cracking of the paste (Marchand 1994, Pigeon 1995).

The third and most recent theory was produced by Litvan, who conducted a large number of experiments to study the behavior of porous materials upon freezing (1960-1980). He noticed

that during the slow cooling period, a large portion of the evaporable water was lost from the porous samples. The basis of his theory is that because of surface forces, the water in the capillary pores cannot freeze in situ, and thus becomes supercooled (Litvan 1978, Marchand 1994, Pigeon 1995).

When the temperature decreases below 32 °F, the vapor pressure over the bulk of the paste, p, corresponds to the vapor pressure of ice because ice will form on all external faces of the paste. The vapor pressure of the supercooled water, p_{ow} in the capillary pores is greater than that of ice. Therefore, the relative humidity for the supercooled water (p/p_{ow}) will be lower than 100 percent and drying will occur. Water contained in the pores will migrate to, and freeze at locations where the effect of the surface is not felt. The radius of curvature of the menisci in the capillaries will decrease as the amount of water decreases. This results in a reduction of the vapor pressure of the unfrozen water because the free energy of a liquid is less when it has a concave instead of planar surface. Equilibrium will be established when the vapor pressure in the capillary pores equals that of ice. Nevertheless, the difference in vapor pressure between ice and supercooled water is greater at lower temperatures, thus the phenomenon will be more severe in that case (Litvan 1978, Marchand 1994, Pigeon 1995).

Litvan attributes the damage of concrete to the following mechanisms: "If a flaw in the solid is surrounded by sound concrete, any water from the undamaged portion will migrate on cooling to the crack, filling it completely; on solidifying, it causes the fissure to propagate. On the following cooling leg of the freeze-thaw cycle, the crack draws more water and freezing results in further damage. Damage also occurs when the required rate of water expulsion (usually necessitated by rapid cooling) is so high that it cannot be realized in the paste. In such cases, some of the passage ways presumably become blocked by ice and internal pressure is generated" (Litvan 1978, Marchand 1994). Although there are several indications that some part of the unfrozen water tends to migrate upon freezing, Litvan's assumption that water cannot freeze in situ has been refuted by many experimental investigations (Marchand 1994, Pigeon 1995).

In conclusion, none of the present theories are able to explain the problem of frost action in its entirety. Each theory describes only certain parts of the overall phenomenon, and thus in a way

they seem to complement each other. Which mechanism will dominate the action of frost in a particular case depends on the characteristics of the concrete and on the conditions to which it is exposed. For example, if the ion concentration in the capillaries is low, the hydraulic pressure will govern, but at high ion concentrations (for example in the presence of deicer salts) it is probably the osmotic pressure that will dominate because the higher the ion concentration the lower the volume of freezable water (Pigeon 1995, Fagerlund 1997).

2.1.1.2 Deicer salt scaling mechanisms

It is generally accepted that there are two distinct types of deterioration due to frost action: internal microcracking and disruption, and surface scaling. Internal cracking leads to little change in weight and appearance, but impacts the mechanical properties, ultimately resulting in complete destruction of the concrete. Surface scaling is characterized by a progressive loss of small cement paste or mortar particles, which in severe cases can be accompanied by the loss of coarse aggregates, potentially affecting the concrete to a depth of 0.5 to 0.75 in, but with little loss of overall strength (Marchand 1994, Pigeon 1995).

The mechanisms causing internal pressure described previously were developed to explain globally the action of frost on hardened cement paste and concrete, but they are also at least partly responsible for surface scaling. The exact causes underlying surface scaling are still not fully understood, but they probably involve more than one process. Also, it is generally accepted that deicer salts amplify the frost action mechanisms described earlier (Marchand 1994, Pigeon 1995, Mindess 2003).

As salt solutions have a lower vapor pressure than water, deicer salts will lower the rate of evaporation of the water contained in the capillary pores, and thus increase saturation of the concrete near the surface where more water will be available for the frost action mechanisms. Powers suggested that the presence of deicer salts in the alkaline pore solution amplifies the osmotic pressures generated when freezing occurs. Litvan explained that as the presence of deicer salts lowers the freezing point of water, it increases the difference between the vapor pressure over the supercooled water in the capillary pores and that over the ice formed on all the external surfaces of the paste (Marchand 1994, Pigeon 1995, Mindess 2003).

Rösli and Harnick (1980) have shown that iced-concrete surfaces can be subjected to an important thermal shock when thawed by means of deicing salts. The large quantity of heat required for phase transformation to occur from ice to water is obtained from the concrete surface, which may result in the creation of a significant temperature gradient. The stress induced in the surface layers by the thermal gradient can surpass the tensile strength of concrete and lead to microcracking. They also suggest that a layer-by-layer freezing could lead to surface scaling. The outer layer of the concrete contains relatively little deicer salts because it is washed out by the liquid water at the surface. In that layer, ice can thus form at temperatures slightly below 32 °F. However, in the layer directly underneath (about 0.5 in from the surface), the salt concentration is high and freezing generally does not occur. This creates stresses due to different expansion of the two layers that can cause scaling (Rösli 1980, Marchand 1994, Pigeon 1995).

The growth of salt crystals is another phenomenon that could contribute to surface scaling. However, it can only occur if the pore water solution reaches supersaturation, which is rarely the case (Pigeon 1995). Deicer salts may also contain sulphates or other deleterious chemicals as impurities, which can increase the risk of other phenomena like sulfate attack, alkali- aggregate reactions, and corrosion of reinforcing steel (Marchand 1994, Pigeon 1995).

Finally, Marchand et al. (1994) suggest that there might be a chemical interaction between the deicing salts and the cement paste hydration products. So far, the mechanisms of scaling deterioration were considered mainly physical, because studies showed that scaling was most important at low salt concentrations (around 3 to 4 percent). However, some reports indicate that the long-term exposure to sodium chloride solutions favors the leaching of calcium hydroxide. The chemical reaction is described as:

$$2NaCl + Ca(OH)_2 \rightarrow CaCl_2 + 2NaOH$$

The calcium hydroxide leaching increases the porosity in the vicinity of the exposed surface, which is likely to enhance the amount of ice formed near 32 °F. Nevertheless, this phenomenon

is not likely to be observed in laboratory testing since the exposure time is too short (Marchand 1994).

2.1.2 The role of air-entrainment on the frost resistance of concrete.

The three frost action mechanisms described earlier all agree that frost damage of concrete results from internal pressures generated by the restrained movement of water, and that a good way to protect the paste is to create a protective network of bubbles by entraining air in the concrete (Marchand 1994, Pigeon 1995, Fagerlund 1997, Ymashita 1997, Mindess 2003,). The present section describes the role played by the air-void system, and the characteristics it needs to have in order to be efficient. The production of the air-void system and the determination of its parameters in hardened cement paste will be described later.

Air is entrained in concrete to create in the paste a protective network of closely spaced air voids. These voids are approximately spherical in shape and range in diameter from 0.05mm to 1.25mm. According to the hydraulic pressure theory and Litvan's theory, the protective effect of the air voids can be ascribed to the fact that since they are larger than the capillary pores, they will rarely be saturated, and thus provide empty spaces within the paste to which excess water can move and freeze without causing damage. However, according to the osmotic pressure theory of Powers, the role of the air bubbles is to compete with the capillary pores where ice is forming. Although the air bubbles are mostly empty, they may have a film solution on their surface that is thick enough to freeze at a temperature near 32 °F. The solution will become more and more concentrated and water will be attracted from the smaller pores where ice forms only at lower temperatures (Litvan 1978, Marchand 1994, Mindess 2003).

Moreover, an indirect effect of air-entrainment is that the tiny bubbles act like fine aggregates in the cement paste, reducing the interactions between solid aggregates. So, they improve the workability and cohesiveness of the mix, and thus facilitate placing and compaction for a given slump. They also considerably reduce bleeding and segregation during handling and transportation of plastic mixes. However, air entrainment introduces additional void space in the paste, and thus reduces the strength of the concrete (around 5 percent loss of strength for each 1 percent increase in air-content). This can be offset by taking advantage of the improved

workability, to reduce the water-to-cement ratio (*w/c*) for a desired slump, and so reduce the capillary porosity. Either way, it is recommended that a low *w/c* should be used for concrete that will be exposed to freezing and thawing (see discussion in section 2.1.5: other factors affecting the frost resistance of concrete) (Pigeon 1995, Mindess 2003).

2.1.2.1 Important parameters of the air-void system

In order to obtain an air-void system that has both the volume capacity and the geometric parameters necessary to protect mature saturated cement paste during exposure to freezing and thawing, a lot of small well-distributed air bubbles are necessary. In other words, the concrete must have an acceptably high air content (A) and a low enough spacing factor ($\bar{L}$) to provide protection (ASTM C457). The spacing factor is considered to be the most important factor with regard to frost resistance since it is "the spacing of the air voids which determines the maximum distance that freezable water must travel through the cement paste to reach an escape boundary where ice crystals can grow freely without generating disruptive pressures" (Pigeon 1995).

The air content must be in the range of 2 to 8 percent by volume of concrete for satisfactory frost protection, with the actual amount dependant to a large degree on the maximum size of the coarse aggregate. It will be higher for lower maximum size of coarse aggregate, because more paste is required to provide workable concrete in that case. For example, the optimum air content for 0.75 in maximum coarse aggregates size is around 6 percent. However, adequate air content is not directly related to an adequate air-void system. High air contents generally indicate larger bubble size rather than a smaller spacing factor. Also, entrapped air voids will be accounted for in the air content (A) even though they don't really have a beneficial effect on the frost resistance of concrete. These voids generally have a diameter over 1 mm, but can reach the size of coarse aggregate particles or larger as a result of poor consolidation. They are irregular in shape and usually have an irregular distribution in the concrete. Finally, excessive amounts of air will drastically lower the strength of the concrete while increasing its permeability. In combination, this will reduce the concrete's resistance to stress produced from freezing (Pigeon 1995, St. John 1998, Mindess 2003).

The most widely used maximum value for the spacing factor is 200μm. However, Pigeon et al. (1995) state that although 200μm should normally be considered as a safe design value for concretes exposed to severe weathering in northern climates, the critical spacing factor for deicer salt scaling resistance will depend on the type of cement and the duration and intensity of the cyclic freezing. For example, this value can be higher for high performance concretes, since they have a higher tensile strength and less freezable water in the capillary pore system. On the other hand, freezing cycles with long freezing periods are more harmful to concrete than cycles with shorter freezing periods. In practice, for lower values of the air-void spacing factor, the performance can be good or bad, since the frost resistance of a given concrete is not just related to its intrinsic characteristics, but also to the conditions that it will be subjected to during freezing. Yet at high spacing factor values, the performance seems always to be bad, even though there is no clearly defined critical value. Also, the critical spacing factor is lower in presence of deicer salts (Pigeon 1995).

Finally, another parameter that is sometimes used to characterize the air-void system is the specific surface area of the air voids, α, which represents the surface area of the air voids divided by their volume (Pigeon 1995). It is related to the bubble frequency and reflects the mean size of the bubbles. In a well developed air-void system, α should not be less than $25mm^2/mm^3$ (Mindess 2003).

2.1.3 Production of the air-void system in hardened concrete

Air is naturally incorporated in fresh concrete by the mixing process. However, the addition of an air-entraining admixture is necessary to stabilize the air bubbles in sizes and spacing that will protect the concrete. The most commonly used chemicals for that purpose are sodium salts of wood resin (vinsol resin), salts of fatty acids, salts of sulphonated hydrocarbon, and alkyl-benzyl sulphonates. The ASTM C 260 Standard pertaining to the acceptance of an admixture as a valid air-entraining agent states that such an admixture should be able to produce an air-void system with a specific surface higher than $25mm^2/mm^3$ and a spacing factor smaller than 200μm at a total air content of 5 to 8 percent (Pigeon 1995).

Most of the air-entraining admixtures contain surface-active agents (surfactants) that concentrate at the air-water interface, and lower the surface tension of the water. Consequently, they reduce the energy required to form the voids and break them down into smaller voids. The natural tendency of small air bubbles in the absence of surfactants is to coalesce to form larger bubbles, because the surface energy (which is equal to the surface tension of the material multiplied by the surface area) of the former is higher, and any system tends towards its lowest value of free energy. However, the surfactants will form an elastic film around the air bubbles that will reduce the risk of coalescence when collisions occur during mixing (Pigeon 1995, Mindess 2003). Indeed, very often, surface-active agents are composed of molecules that have a negatively charged hydrophilic (water-loving) end and a hydrophobic (water-hating) end. These molecules therefore tend to align at the air-water interface with their hydrophilic groups in the water (adsorbed to the cement grains) and the hydrophobic portion in the air, thereby effectively binding the air voids to the cement grains (Pigeon 1995, St. John 1998, Mindess 2003).

A typical dose for air entraining agents is only 0.005 to 0.05 percent of active ingredient by mass of cement. Higher dosages should increase air content and decrease bubble size in fresh concrete; however, varying results will be obtained depending on the job conditions. Air entrainment occurs while the concrete is being mixed, therefore the type and time of mixing is important. Optimal air content is obtained with normal mixing time, whereas air loss can occur during extended mixing or vibration. Normally, the mixing time should be increased for larger batches in a given mixer, or for less efficient mixers (Mindess 2003).

The viscosity of the cement paste is also an extremely important parameter. For stiffer concrete (higher viscosity), more energy is required for mixing, but the risk of coalescence of the air bubbles is reduced. A more viscous paste also usually contains more solid particles (or finer particles) for a given amount of water, so that less water will be available for the formation of air bubbles since all solid surfaces need to be covered with water (Pigeon 1995).

Consequently, at a given dose of air entrainer, lean concretes (more aggregates, less paste) entrain less air than do rich mixes, and low *w/c* ratio concretes entrain less air than do concretes with high *w/c* (Pigeon 1995). However, for a given air content, low *w/c* ratio concretes tend to

have a lower spacing factor than high *w/c* concretes. Since finer particles have a higher specific surface, the air content for a given dosage will also vary inversely with the proportion of fines in the fine aggregate, the addition of finely divided mineral admixtures (e.g. silica fume, fly ash, ground blast furnace slag, natural pozzolans, etc.), and the fineness of the cement. Finally, the amount of air for a given dosage of air entraining agent will also decrease as the temperature increases, because of the loss of slump at higher temperatures (Pigeon 1995, Mindess 2003).

The use of other admixtures simultaneously with air-entraining agents may have positive or negative effects on air entrainment. Water-reducers and superplasticizers usually reduce the amount of air-entraining agent required to obtain a given air content, because they increase the fluidity of the paste and thus tend to enhance the effect of air-entraining agents. However, they do not increase the stabilizing effect of the air-entraining agent, and thus may have a detrimental outcome on the stability of the system resulting in an increased spacing factor. The use of retarding agents does not seem to have a very significant effect on air entrainment, except that it prolongs the time during which the air-void system can change. Although the system probably doesn't change much after casting since there is no energy input (Marchand 1994, Pigeon 1995, Mindess 2003).

Impurities in the mixing water or in the aggregates may have a positive or negative effect on air entrainment. For example, calcium carbonates, which are known to reduce the capacity of water to dissolve soaps and detergents, could negatively affect air entrainment. In the same way, fly ash or silica fume that contain a significant amount of carbon can create severe air void production and stability problems, because carbon slowly inhibits the air-entraining admixtures and thus gradually reduces the amount available for air-entrainment (Pigeon 1995, Mindess 2003).

Significant loss of air content can occur between original mixing and final placement. However, coarse bubbles are selectively eliminated, and only extended vibration will remove a sufficient number of the fine bubbles that will compromise frost resistance (Pigeon 1995, St. John 1998, Mindess 2003). Surface-finishing operations can also influence the air-void system characteristics of the surface layers. Overworking in particular, can increase the value of the air-

void spacing factor in the surface layer and thus increase the risk of surface scaling (Marchand 1994, Pigeon 1995).

Finally, the air-void system of hardened concrete can also degrade over time if some air voids become filled with secondary deposits. The most common deposit in voids and cracks is secondary ettringite, which usually results from leaching through the percolation of water. It is formed by precipitation from solution of primary ettringite, a common component of hydrated cement paste that is formed during the hydration process from the reaction of tricalcium aluminate (C_3A) with gypsum and water (Mindess 2003, Sutter 2001). "Over time the incremental deposition of ettringite and other secondary deposits on the walls of the air voids may completely fill the interstitial pore space and air-void system, leaving the concrete vulnerable to freeze-thaw deterioration"(Sutter 2001).

It is obvious from this discussion that, considering the large number of parameters that affect the production and stability of the air voids, testing is the only way to verify whether the use of a particular air-entraining admixture in a given mix will yield a system of closely spaced air voids that will remain stable until the concrete has set. Also, once the dosage of the air-entraining agent required to obtain a correct spacing factor for a given mix is determined, no mix parameter should be changed significantly, because a change may result in a higher spacing factor even if the air content stays constant. (Pigeon 1995).

2.1.4 Characterization of the air-void system in hardened concrete

The most common way to characterize the air-void system of an existing structure is to obtain samples of hardened concrete and subject these to a microscopical examination. However, prior to computing the parameters of the air-void system, careful sample preparation is required in order to provide a perfectly planar and smooth surface where the air voids and the aggregates can be clearly distinguished from the cement paste. Sutter (2001) and Van Dam (2002a) give a good description of the different steps of the sample preparation.

2.1.4.1 Test procedure and computations of the air-void characteristics

The major parameters used to determine the susceptibility of hardened concrete to damage by freezing and thawing are: air content, specific surface, void frequency, spacing factor, and paste-air ratio. ASTM C457-90 is the most widely used method for the microscopical determination of these parameters.

This test method describes two procedures to examine the finely ground specimen surface under a high quality stereoscopic optical microscope: the linear traverse method, and the modified point-count method. In the present study, the modified point count method was used and thus will be described.

In the modified point count method, the polished concrete slab is viewed through a stereo microscope at a magnification between 50X and 150X. A grid is then applied virtually to the prepared surface and the operator records for each intersection (each stop of the stage) if the point is located at an air void, an aggregate, or cement paste. In addition, the number of air voids intercepted by the horizontal lines of the grid, the lines of traverse, is also recorded. The standard stipulates a minimum required examination area, traverse length and number of points depending on the maximum aggregate size (ASTM C457, Pigeon 1995, Peterson 2001).

The raw data obtained from the application of the modified point count method are as follows:

S_a=number of stops in air voids
S_t=total number of stops
N=total number of air voids intersected
S_p=number of stops in paste
I=the E-W translation distance between the stops

Once recorded, these values are then used to calculate the parameters of the air-void system. Peterson (2001) gives a good overview of the theories underlying the following calculation:

Air content (A) - the proportion of the total volume of the concrete that is air voids; expressed as a percentage by volume:

$$A = \frac{S_a \bullet 100}{S_t} \qquad (2.1)$$

Paste content (p) – The proportion of the total volume of the concrete that is hardeneded cement paste, expressed as a percentage by volume:

$$p = \frac{S_p \bullet 100}{S_t} \qquad (2.2)$$

Void Frequency (n) - the voids per unit length of traverse:

$$n = \frac{N}{T_t} \qquad (2.3)$$

where T_t is the total traverse length=$S_t I$

Specific surface (α) – the surface area of the air voids divided by their volume

$$\alpha = \frac{400n}{A} \qquad (2.4)$$

Spacing factor ($\overline{L}$) – average distance from any point in the paste to the edge of the nearest air void:

If p/A is less than or equal to 4.342

$$\overline{L} = \frac{p}{400n} \qquad (2.5)$$

if p/A is greater than 4.342

$$\overline{L} = \frac{3}{\alpha}\left[1.4\left(1+\frac{p}{A}\right)^{1/3} - 1\right] \qquad (2.6)$$

2.1.4.2 Precision of the measurements

The precision of the microscopical determination of air-void characteristics may be expected to be subject to the reasonably predictable statistical errors associated with any counting technique, but in addition they will be affected by many other parameters, such as the microscope magnification, the quality of the prepared specimen, the sample size, and the performance of the operator (St. John 1998, Pigeon 1995). So, it is difficult to assess theoretically the precision of this measurement.

However, a study done on more than 600 air-entrained concretes (Pleau et al. 1992) indicates that the maximum error associated with the determination of the three most important parameters of the air-void system (air content, specific surface of air voids, and air void spacing factor) decreases exponentially with the number of slabs examined. Pleau found that when the minimum requirements of the ASTM C 457 Standard are strictly satisfied for a nominal maximum size aggregate of 0.75 in (which was the case in the present study), the maximum error of the microscopical examination is evaluated at approximately 28 percent, 20 percent and 16 percent for A, α, $\overline{L}$, respectively. The study also underlines the fact that A is less accurate than α, which is less accurate than $\overline{L}$. This can be explained by the fact that the accuracy increases with the numbers of parameters involved in the computation because one is unlikely to obtain, simultaneously, a large error in all parameters (Pigeon 1995).

ASTM C457 also contains a section on the precision and bias associated with the determination of the air-void system parameters. A study was done on the determinations made on a series of four lapped specimens prepared in one laboratory and then circulated to nine different laboratories. In general, the coefficient of variation found was around 12 percent for the determination of the spacing factor and between 8 and 15 percent for the determination of the air content. The standard underlines that the variability would be higher in actual practice for specimens sampled and prepared from in-place concrete (which is our case) since additional variation due to sample selection and surface preparation in different laboratories would increase the coefficient of variation.

Finally, the air content parameter has to be considered with some skepticism. As described by St. John et al (1998): "sources of apparent contradiction between air content findings and actual performance include the type of air voids and the spacing factor". In ASTM C457, no distinction is made regarding the nature of the air void when recording whether the point is located over an air void, an aggregate or cement paste. So, a high air content can be due to the presence of entrapped air voids, or porous aggregates rather than to multiple entrained air voids, although only the later will protect the paste against frost action. However, only the entrained air voids are considered when recording the voids intercepting the traverse line, so once again the spacing factor is a better indicator of the adequacy of the air-void system (Pigeon 1995, St. John 1998).

2.1.5 Other factors influencing the frost resistance of concrete

Concrete is a heterogeneous material, so its frost resistance will be a function of both the characteristics of the aggregates and the properties of the cement paste. The influence of the aggregates can be very important, since they represent about 75 percent of the total volume of the concrete. However, only the factors affecting the resistance of the cement paste will be treated in this paper, because contrary to the aggregate characteristics, they can be modified according to the known durability criteria (Pigeon 1995).

The *w/c* is a very important parameter influencing the durability of concrete. Lowering *w/c* not only decreases the volume and the size of the capillary pores, it also increases the strength of the paste. The pore size distribution has a direct effect on the volume of freezable water and thus on the frost resistance of concrete. Smaller pores not only result in a more impermeable concrete, with less chance of saturation and better overall resistance to aggressive agents (like deicer salts), but also lowers the temperature at which the water in the pores will freeze, since the smaller the size of the pore, the higher the surface forces (Marchand 1994, Pigeon 1995, Mindess 2003, Ymashita 1997). Thus, the lower the *w/c*, the higher the spacing factor required for good frost resistance. Pigeon et al. (1995) state that from the data available at present time, air entrainment is generally not required for high-strength concretes having a *w/c* ratio lower than about 0.25. However, it is clear that air entrainment is needed for concretes having *w/c* higher than 0.35.

A study done by Stark et al. (1997) seems to indicate that not only the amount of water, but also the water quality has a considerable influence on the frost resistance of concrete. Water from three different drinking water supply sources was used in the study, covering the whole range of hardness from very soft to very hard. The test results show that scaling proceeds in the same way, regardless of the water used, but that the amount of scaling increases with the increasing degree of hardness of the water. Moreover, the effect of the water quality is even greater with concrete containing blast furnace slag cement. Nevertheless, the explanation of these experimental findings does not exist at this time and the influence of the water quality in the presence of deicer salts has not been examined (Stark 1997).

The published data concerning the use of supplementary cementing materials, like fly ash, blast furnace slag, and silica fume in concrete subjected to freezing and thawing are often contradictory. The use of these materials usually decreases the capillary pore size distribution, and thus the permeability of the paste and the amount of freezable water, but not the total capillary pore volume. If the reduction in permeability is more important than the reduction in the amount of freezable water, the resistance of the concrete against freezing may decrease, because a less permeable paste offers greater resistance to the flow of water being forced out of the capillaries during freezing, and the internal disruptive pressures caused by this flow are thus increased (Marchand 1994, Pigeon 1995). Moreover, the use of these materials usually also results in more brittle cement paste matrix. In all cases, Marchand (1994) suggests that the use of supplementary cementitious materials in the production of concrete elements exposed to freezing and thawing cycles should be considered with caution.

ACI standard 318 gives some limits on water-to-cementitious materials (*w/cm*) ratio instead of *w/c* for durability on various exposure conditions involving freezing and thawing. However, according to Johnston (1994) performance appears unrelated to *w/cm* ratio and instead quite closely related to *w/c*. Tests show that concretes with fly ash or silica fume as part of the cementitious materials behave very differently from each other and from the concrete made with only portland cement as the binder. Fly ash concretes generally scale severely even when *w/cm* is well below the code maxima of 0.45, and show a strong correlation between degree of scaling and *w/c* rather than *w/cm*. However, the traditional *w/c* limit of 0.45 is associated with

satisfactory scaling resistance for properly air-entrained concretes containing cement alone. Therefore, Johnston (1994) recommends taking the code limits as *w/c* instead of *w/cm*.

The use of accelerators, retarders and other admixtures usually has little effect on the frost durability and the pore structure of concrete. Nevertheless, as mentioned previously, they can influence the air-void system. Moreover, the use of retarders and water reducers at high dosages can significantly increase bleeding (Marchand 1994, Pigeon 1995). Excessive bleeding has a harmful effect on concrete durability because it produces defects such as water channels and water pockets beneath the aggregates originated by the up flow of water. It also causes segregation and increases the *w*/c and the porosity near the surface of the concrete and consequently reduces the frost and scaling resistance of the concrete (Marchand 1994, Pigeon 1995, Shoya 1997).

The type of portland cement can also have an impact on the durability of concrete exposed to freezing and thawing cycles, since it affects the capillary porosity and the tensile strength of the paste. Cements with a higher fineness have been found to provide a better resistance to frost action because they lead to a finer pore size distribution, although they make air-entrainment more difficult and thus higher dosages of air-entraining agent should be used. The cement content is not, per se, an important parameter with regards to scaling resistance. However, for a given aggregate quality, lower paste content means a concrete with lower porosity and with better mechanical properties (as long as they have an adequate *w/c* and that their workability is sufficient to allow proper consolidation) (Marchand 1994).

The capillary porosity of the hardened cement paste and thus the frost resistance of the concrete, are also greatly influenced by the curing procedure. Since the curing procedure mostly affects the surface layer of the concrete its influence on surface scaling is even greater. Furthermore, if curing procedures are delayed, plastic shrinkage cracking can occur, allowing water to penetrate quickly into the concrete, enhancing the potential for freeze-thaw attack, and significantly reducing the surface durability (Marchand 1994). For low *w/c* concrete, water curing is better than sealed curing since it protects the concrete against self-dessication (Mindess 2003).

Curing at high temperatures (140 °F) has also been found to be very detrimental to the scaling resistance of certain types of concretes especially because it usually results in a coarser pore structure and consequently more ice forming at temperatures near 32 °F (Marchand 1994, Jacobsen 1997). However, according to a study conducted by Jacobsen et al., the effect of high curing temperatures on the amount of ice formation seems to decrease with lower *w/c* and with the addition of silica fume (Jacobsen 1997).

Sometimes, sealers are used as an impervious coating on the surface of the concrete in order to prevent the ingress of chloride ions and moisture. Though studies show that this practice only slightly increases the resistance to freeze-thaw damage of concrete with a poor air-void system, for well air-entrained concrete the opposite is true. After a certain number of freezing and thawing cycles, the concrete generally suffers a sudden deterioration. At the conclusion of the testing the damage is usually greater than in the absence of a sealer. This is because the sealer completely prevents moisture movements, so that moisture tends to accumulate in the concrete just underneath the coating, and subsequent freezing completely disrupts the paste matrix. When the sealer is applied on a surface that has already been contaminated with deicer salts, the little positive effect it had for poorly air-entrained concretes is reduced, and the negative effect on the well air-entrained concretes is even more pronounced (Marchand 1994, Hazrati 1997).

2.1.6 Summary of background on freeze-thaw durability

Over the years, several attempts have been made to explain the damage caused to concrete by freezing with and without the presence of deicing chemicals. However, the mechanisms underlying frost action and deicer salt scaling are very complex and are still not fully understood. The frost resistance of concrete seems to be influenced by many factors, although it is generally accepted that the use of an adequately air-entrained, low *w/c* concrete is the best protection. The best method for assessing the air-void system is the application of ASTM C 457, which is based on the stereo optical evaluation of a polished concrete surface.

2.2 Alkali-Silica Reactivity (ASR)

Alkali-silica reactivity (ASR) is a distress that results from an expansive chemical reaction between alkalis contained in the pore solution of a concrete and certain reactive forms of silica within the aggregate (St. John 1998, Sutter (2001)).

2.2.1 Manifestation of distress due to ASR

The rate of the alkali-silica reaction can be very low and depends on several factors including the amount of alkalis in the concrete, the amount and type of reactive silica, the temperature, and availability of moisture, so evidence of ASR in a concrete structure may sometimes not be seen for years and is usually not uniform across the surface (concrete exposed to a warm and humid environment or to repeated cycles of wetting and drying are more vulnerable). The manifestation of ASR in a concrete structure can vary from just one or two isolated cracks to large areas of polygonal pattern cracking (map-cracking), which tend to align perpendicular to the direction of least restraint since expansion of a concrete element tends to occur in that direction. In some cases, the expansion of the concrete due to ASR can lead to the closure of expansion joints or the misalignment of structural elements. Other less common features that can be observed are exudation of reaction products (alkali-silica gel), pink-brown coloration along the margins of cracks (due to alkali bleaching the lichens which may be present on the concrete surface), and popouts (breaking away of small conical fragments of the concrete) (St. John 1998, ACI 1998).

2.2.2 General mechanisms of ASR

ASR can only proceed and be sustained if the following three conditions are satisfied:

1. High pH in the pore solution surrounding the particle - The first step in the reaction process is the depolymerization and dissolution of reactive silica. Silica is relatively insoluble in neutral and acidic environments, but its solubility strongly increases at higher pH, so significant attack will only occur at the upper end of the pH range. Consequently, a high percentage of alkalis must be present in the concrete to release hydroxil ions in the pore solution (higher pH) in order to dissolve the reactive silica (St. John 1998, ACI 1998, Helmuth 1992, Lane 1992). Usually, the principal source of alkalis is derived from the cement itself, but any source of sodium or potassium (internal or external) can contribute to the reaction provided that the alkali can move

into the pore solution of the concrete and create the necessary hydroxil ion concentration required. Aggregates, ground water, seawater, chemical and mineral admixtures, industrial solutions (for example fertilizers), and deicing salts (e.g. sodium chloride) may be potential sources of alkalis (Helmuth 1992, ACI 1998, St. John 1998, Mindess 2003, FHWA 1997).

2. *Sufficient moisture is present in the pore structure of the concrete* - For ASR to proceed, the internal relative humidity of the concrete must be above 80 to 85 percent. Indeed, enough water is necessary to transport the alkali and hydroxil ions to the sites of reactive silica. As silica is attacked by the hydroxil ions and is in the process of dissolution, it will swell; however, usually this is not significant enough to cause cracking. Once the reactive silica is dissolved it will react with the potassium and sodium hydroxide to form alkali silica gel. It is the absorption of pore solution by that gel, and its subsequent swelling that will generate pressures large enough to cause cracking within the aggregate particle and then subsequently cracking of the paste matrix surrounding it (Helmuth 1992, St. John 1998, ACI 1998).

3. *Reactive minerals in the aggregate* –There are only two generalized classes of minerals that are known to be expansively reactive with the alkalis in the concrete: metastable types of silica (including some disordered forms of quartz), and alumino-silicate glasses with a silica content usually in excess of 60 to 65 percent and not less than 50 percent. The natural forms of the metastable silica are opal, chalcedony, tridymite, cristobalite, quartz, and of the alumino-silicate glasses the matrix of fresh intermediate to acidic volcanic rocks. Also, most commercial glasses including fibers and mineral wools are reactive (St. John 1998). The reactivity of the various forms of silica depends on the degree of crystallinity, the crystal size, internal porosity, and internal crystal strain. In general, crystalline forms of silica, unless they are highly strained, are less reactive than amorphous and porous ones, because they are less susceptible to dissolution by high pH medium (St. John 1998, Mindess 2003).

In many cases, the reactive mineral is dispersed in the rock texture and forms only a small part of the aggregate (can be as low as 1 percent); however, not all aggregates containing those minerals will be susceptible to alkali-silica reactivity. Maximum expansion occurs when the aggregate has a particular percentage of reactive silica (the "pessimum percentage"). That percentage depends on the form of the reactive silica, the degree of alkalinity, and the *w/c*. Up to the pessimum percentage (at low silica to alkali ratio) an increase in the amount of reactive silica produces an

increase in total reaction product and thus an increase in expansion. However, if the percentage of silica in the aggregate increases past the pessimum percentage, the ratio of silica to alkalis gets so high that a lot of the alkali is absorbed and the concentration of hydroxide in solution is insufficient to maintain the same severity of attack, thus the expansion decreases (St. John 1998, Mindess 2003).

The reactivity of an aggregate (whether it reacts quickly or slowly), and the amount of alkalis in the concrete necessary to cause it to react, will not only depend on the composition, but also on the geologic origin and textural characteristic of the rock from which it is derived. The reactivity of an aggregate tends to increase with increasing porosity and decreasing size, since the rate of access of the pore fluid to the reactive minerals in the aggregate increases in those cases (St. John 1998, ACI 1998).

2.2.3 Measures to prevent alkali-silica reactivity (ASR)

In order to avoid ASR, at least one of the three previously mentioned conditions must be controlled, that is: controlling the type and amount of reactive silica, lowering the moisture content of the concrete, or lowering the pH of the pore solution by lowering the amount of available alkalis.

The best way to prevent ASR is to avoid using susceptible aggregates, based on petrographic analysis and field service records (ACI 221 recommends that the evaluated structure should be at least 10 years in service and have the same material composition, mixture proportions, and service conditions as the projected structure) (ACI 1998, Stark, J 1997). However, aggregates are becoming scarce in many regions, so avoiding the use of susceptible aggregates in not always economically viable. In some cases, the problem can be solved by using some aggregate beneficiation strategies, like chemical treatments or dilution (blending reactive with non-reactive aggregates), but that is not applicable in every situation (ACI 1998).

No expansion will occur if the relative humidity in the pore structure of the concrete is below 80 to 85 percent (ACI 1998, Helmuth 1992). However, such a low relative humidity can practically

only be attained in interior concrete in buildings, or in concrete in very dry climates (only if the concrete is not in contact with the ground), and even in those situations, structures with large cross-sections may take a long time to become completely dry. It is thus in most cases difficult to reduce the relative humidity of the concrete enough to completely prevent deterioration caused by ASR, but some measures can be taken to reduce the permeability of concrete to external moisture, and at the same time to external sources of alkalis (like deicer salts), to reduce the potential for expansion.

A low *w/c* is commonly known to reduce the porosity (permeability) of the concrete, and the amount of water initially present in the pore structure, although it will only delay the expansion caused by ASR or in some cases even aggravate it. Indeed, since at low *w/c* less water is initially present in the pores, the alkali concentration of the pore solution tends to be higher. Moreover, the reduction in porosity also results in a reduction of the space available to accommodate the expansion of the alkali-silica gel (ACI 1998).

Pre-existing cracks increase the permeability of the concrete, creating an entry point for sources of external alkalis and water. Consequently, cracking due to frost-action, shrinkage cracking, and all other forms of cracks may initiate or aggravate ASR (Helmuth 1992, Guedon 1994). Adequate curing is thus very important, not only because it reduces the porosity and improves the strength of the concrete, but also because it reduces shrinkage cracking. An adequate air-void system will protect the concrete against frost-action, and will also delay the expansion caused by ASR by providing empty spaces for the alkali-silica gel to expand into. A study done by Collins et al. (1986) tends to indicate that the expansion can also be reduced by the use of porous aggregates, since these also provide empty spaces for the alkali-silica gel, but possibly also because the water absorbed in the aggregates dilutes the potassium ion in the pore water, reducing the potential for reaction (St. John 1998).

Pozzolanic materials like raw or calcined pozzolans, fly ash, rice husk ash, silica fume, metakaolin, and granulated blast furnace slag (GBFS) are commonly used as partial cement replacement to reduce the potential for excessive expansion of concrete by ASR. These materials protect the concrete against deterioration by ASR in several ways:

- When used as partial cement replacement, they reduce the total alkali contribution of the cementitious materials, since most have lower alkali content than cement (Helmuth 1992, ACI 1998, Mindess 2003).
- These materials are mostly composed of amorphous or glassy silica, which reacts with the calcium hydroxide (CaOH) formed from the hydration of the calcium silicates to form a calcium silicate hydrate (C-S-H) gel with a lower $CaO:SiO_2$ (C/S) ratio than the C-S-H gel formed in regular cement hydration. This C-S-H gel has a greater capacity to entrap alkalies and reduce the pH of the concrete pore fluid (Helmuth 1992, ACI 1998, Mindess 2003).
- ASR gel that forms in a paste with reduced amounts of CaOH may have lower swelling characteristics (Helmuth 1992, ACI 1998, Mindess 2003).
- They reduce the permeability of the concrete by lowering the amount of CaOH (which has a tendency to leach out over time, increasing the porosity of the concrete) and by increasing the amount of C-S-H gel, and thus reduce the ingress of moisture and alkalies (ACI 1998, Mindess 2003).

The effectiveness of pozzolans and GBFS in reducing the potential for ASR, and the proportions in which these materials should be used as cement replacement depend on the particular pozzolan, the reactivity of the aggregate, and the alkali content of the portland cement. Since the composition of those materials are quite variable, the effectiveness of a particular cement-pozzolan or cement-slag combination should be tested prior to use, but in general the higher the reactivity of the aggregate and the higher the alkali content of the cement, the higher the percentage of pozzolan or slag that should be used as cement replacement (ACI 1998). Also, mineral admixtures with high amorphous silica content, and with high surface area (smaller particle size) tend to be more effective in preventing ASR and thus require smaller proportions. For example, cement replacement values of 5 to 15 percent are common in the case of silica fume (85 to 98 percent silica content), but for slag (32 to 38 percent silica content) replacement quantities of 50 percent are commonly used. Under any conditions, it is important to use a sufficient quantity of pozzolan to adequately convert calcium hydroxide to calcium silicate hydrate. Therefore, special care should be taken when using class C fly ash, because the lime and silica present in the fly ash react with each other, lowering the amount of silica available to

control the alkali-silica reaction. In addition, some class C fly ashes also have a relatively high alkali content. Consequently, it is generally not recommended to use class C fly ash in ASR mitigation, and if used, a cement replacement of at least 35 to 40 percent is required, or the expansion may be increased (Lane 1992, Mindess 2003).

One of the most common procedures to reduce the potential for deleterious ASR deterioration is the use of low-alkali cement. The two main alkali constituents present in portland cement are sodium and potassium oxide. Therefore, the total alkali content of the cement is usually expressed as equivalent Na_2O (Na_2O_e), which is calculated as percent Na_2O plus 0.658 x percent K_2O (ACI 1998, Mindess 2003). Cement with a total alkali content lower than 0.6 percent Na_2O_e is generally recommended when using potentially reactive aggregates (Lane 1992, ACI 1998, Mindess 2003, FHWA 1997). However, it will not prevent deterioration caused by ASR in all cases; indeed, several cases have been reported where the use of cements within that range of alkali content have produced ASR-related expansion in concrete (ACI 1998, Lane 1992). This is partly due to the fact that the hydroxil ion concentration (and therefore the pH) of the concrete pore solution depends on the total alkali content of the concrete, and not only on the alkali content of the cement.

Therefore, some authors suggest a limit of 3 kg Na_2O_e per cubic meter of concrete rather than a limit on the alkali content of the cement (FHWA 1997, Mindess 2003). However, since the actual hydroxil ion concentration required to cause ASR depends on various factors, for example the susceptibility of the reactive silica or the availability of moisture, this limit might also not be broadly applicable. Fournier et al. (Fournier 1999) proposed some guidelines for prevention of ASR in new concrete structures, giving different limits on the total alkali content of the concrete depending on the degree of alkali-silica reactivity (based on one-year expansion in the concrete prism test) and on the level of risk of ASR (based on the moisture conditions and the type of structure). For most situations, they also recommend the use of supplementary cementitious materials in appropriate amounts.

The solubility of the alkalis present in the concrete is also an important factor, since cyclic wetting and drying, freezing and thawing, as well as electrical currents can cause alkali migration

and concentration in concrete. So, a given total alkali content might be tolerable if homogenously distributed, but cause ASR if concentrated at one location in the structure. A study conducted by Dobie (1986) indicates that the use of low-alkali cement might be unwarranted in preventing alkali-silica popouts if water-soluble alkalis are not significantly lowered. Indeed, the formation of popouts due to ASR is accompanied by high concentrations of alkalis at and just below the slab surface. The increase in alkali concentration at the surface of the concrete results from soluble alkalis that are left behind after mixing water evaporates, and is favored by excessive bleeding, hot windy placing conditions (rapid surface drying), excessive troweling, and sealing of the surface after finishing. The source of soluble alkalis is, of course, not limited to the cement; the contribution of the other sources of alkali (e.g. aggregate, admixtures, water, etc.) must therefore be taken into account. Especially, the contribution of class C fly ash is of increasing concern, as the alkalis it contributes may exceed the contribution of the cement (Dobie 1987).

Finally, the use of some ASR-inhibiting admixtures has been shown to be effective in reducing ASR expansion. Although a lot of those are still in the research state, the use of lithium salts appears very promising for ASR mitigation by preventing the formation of additional gel (ACI 1998).

2.3 Ettringite

The section provides a brief overview of some aspects related to the occurrence of ettringite in concrete, discussing primary ettringite, sulfate attack, delayed ettringite, and secondary ettringite that infills the air-void system. This discussion is very brief and the reader is directed to the cited references for more information.

2.3.1 Primary ettringite

Ettringite is a crystalline calcium sulfoaluminate hydrate formed during early hydration of hydraulic cement by the reaction of sulfate ions provided by the added gypsum, and aluminate ions released from the aluminate clinker phase (tricalcium aluminate) (St. John 1998, Famy 2001, Van Dam 2002a, Mindess 2003). The hydrate is only stable while there is an ample supply of sulphate ions. In most cements there is not sufficient gypsum to supply sulfate ions for the formation of ettringite from all available aluminate ions, thus part of the ettringite is usually

converted to another calcium sulfoaluminate hydrate containing less sulfate (monosulfate) within 12 to 36 hours of hydration.

2.3.2 Sulfate attack

The monosulfate can convert again to ettringite when the concrete is brought into contact with a new source of sulfate (e.g.seawater, groundwater, industrial wastes, dissolution of sulfate from the aggregates, etc.). Since the formation of ettringite is an expansive reaction (up to 55 percent increase in solid volume), the conversion can generate internal stresses that ultimately lead to cracking of the concrete (Sutter 2001, Van Dam 2002, Mindess 2003). The resulting distress mechanism, which is a common form of chemical attack of concrete, is referred to as sulfate attack.

2.3.3 Delayed ettringite

Another less common type of distress related to ettringite is delayed ettringite formation (DEF), which occurs primarily in concretes cured at elevated temperature (140 to 200 °F) (Scrivener 1996). At high curing temperatures the sulfate as well as the aluminate ions appear to be absorbed by the C-S-H, so that the formation of ettringite and the associated increase in volume occurs after the concrete has hardened (Mindess 2003). According to Mindess et al. (2003), DEF is usually limited to cases in which the cement has an SO_3 to Al_2O_3 ratio above 0.5, and the concrete is exposed to significant moisture. Also, it appears that the expansion resulting from DEF is only deleterious in the presence of another form of deterioration, like ASR or thermal gradient (Mindess 2003, Famy 2001).

2.3.4 Secondary ettringite

Although, ettringite lining or filling voids or cracks is one of the symptoms of sulfate attack; if no other signs of sulfate attack (e.g. peripheral cracks or gaps around the aggregates as a result of the expansion) are observed, it is more likely that the infilling is simply the result of dissolution and recrystallization of primary ettringite (ettringite formed during early hydration). Indeed, as mentioned by Famy (2001), "the small crystals of ettringite that form in the paste are inherently unstable relative to larger ones because of their greater specific surface areas, and assuming that the water needed for transport is present, the ettringite will recrystallize in cavities or cracks of any sort that may be available." The ettringite that precipitates in the available space is often

referred to as secondary ettringite (SE). Most authors believe that the secondary recrystallization of ettringite does not cause expansion, and is not itself a primary cause of crack formation or propagation; however, the infilling of the air-voids may greatly compromise the freezing and thawing durability of concrete as well as its deicing salt resistance (Ouyang 1999, Stark 1999, Detwiler 1999, Famy 2001). Also, the dissolution and precipitation of ettringite implies that the air voids are water-accessible and often indicates a degree of leaching (St. John 1998, Ouyang 1999). Therefore, since the migration of water is facilitated in distressed concrete, the formation of SE is often initiated by other deterioration mechanisms (e.g. shrinkage cracking, ASR, freeze-thaw attack, etc.) (Johansen 1993, Ouyang 1999, Van Dam 2002a, Famy 2001).

2.4 Carbonation

Carbonation of hardened concrete is caused by the reaction of calcium hydroxide or cement hydrates with atmospheric carbon dioxide. It has both a beneficial and a detrimental effect on the durability of regular portland cement concrete and the corrosion of the embedded reinforcing steel (Hunt 1962, St. John 1998).

2.4.1 Effects of carbonation

Carbonation can be deleterious as the reaction produces calcium carbonate and water, and thus reduces the pH of the pore solution. If the pH drops below 11.5, the passive iron oxide layer that protects the steel reinforcement is destroyed. Consequently, corrosion of the steel will readily occur when the depth of carbonation exceeds the thickness of the concrete cover (Ho 1987, St. John 1998, Mindess 2003). Moreover, hardened cement paste that undergoes carbonation shrinks. The shrinkage can cause cracking of the paste if the carbonation occurs after the concrete has dried and the depth of carbonation is abnormally high (St. John 1998).

On the other hand, calcium carbonate has a molecular volume that is 11 percent greater than the calcium hydroxide it replaces, but 2.5 percent smaller than the cement hydrates. As a consequence of the net increase in volume, the calcium carbonate will fill previously empty pores, improving the strength of the paste and reducing the porosity. However, the reduction in permeability is usually insufficient to prevent oxygen and chloride ions from penetrating to the reinforcement (St. John 1998).

Carbonation of the outer layers of the concrete starts almost as soon as the concrete starts to harden and superficial drying of the surface occurs. However, in a well-compacted, dense concrete the depth of carbonation rarely exceeds 2 mm, even after several years of exposure. Therefore, the carbonation depth is useful to any investigation of the quality and the permeability of the concrete. When the carbonation depth is greater than 2 mm, it is often an indication that the concrete is of lesser quality, and past 5 mm that the outer layer of the concrete is abnormally porous (Ho 1987, St. John 1998).

2.4.2 Factors influencing the depth of carbonation

The depth of carbonation depends on many factors including the quality of the concrete and the conditions of exposure (Ho 1987). The dominant factor is porosity of the paste, as stated by St. John (1998): "Any factor which increases the permeability of a concrete to carbon dioxide will also increase the rate of carbonation providing the necessary internal moisture conditions are present". The rate of carbonation is thus mainly influenced by the *w/c*, as it affects the porosity of the concrete (Hunt 1962, Ho 1987, St. John 1998). However, in the case of poor compaction, which leads to an increase in *w/c* in the outer layers, there may be poor correlation between depth of carbonation and overall w/c (St. John 1998).

Carbonation will also often act in concert with other destructive mechanisms, since cracks create a pathway for carbon dioxide in the concrete, enabling carbonation to penetrate deep into the paste (St. John 1998, DePuy 1994, Mindess 2003). The effect of the cracks will be more important as the crack width increases, and as the quality of the concrete is lowered (St. John 1998). Also, the degree of curing will strongly affect the carbonation depth since it influences the paste porosity and shrinkage cracking. A study conducted by Ho et al. (Ho 1987) showed that the carbonation decreases as moist curing is extended from one to seven days, but remains practically unaffected when curing is prolonged beyond that point.

Moreover, moisture is an important factor in carbonation. The reaction will not occur when the concrete is saturated, because then the water acts as a barrier to the rapid movement of gas. However, a certain amount of water is necessary for reaction to take place since carbonation acts

through solution. Therefore the rate of carbonation is at a maximum when the relative humidity of the concrete is around 50-70 percent (Ho 1987, St. John 1998, DePuy 1994).

Finally, supplementary cementitious materials seem to have, in some cases, a deleterious effect on carbonation. For example, Ho et al. (1987) compared mixes based on common 28-day strength, binder content and *w/cm* ratio and found that fly ash concretes have a lower resistance to carbonation than regular portland cement concretes. The study also demonstrated that regardless of the constituents, the carbonation depends mainly on the *w/c* ratio and not on the *w/cm* ratio (Ho 1987). Also, in the case of blast furnace slag cements, carbonation may have more deleterious effects on the paste, as it appears to decrease strength and increase porosity (St. John 1998).

Chapter 3. Experimental Procedure

The general approach to concrete analysis used in this study was based on the FHWA report entitled, "Guidelines for Detection, Analysis, and Treatment of Materials-Related Distress in Concrete Pavements – Volume 2 (Van Dam 2002b)." Only a summary of the experimental procedure and sample preparation is given here; more details can be found in the above-mentioned document, in Concrete Petrography (St. John 1998), or on the following website http://www.tfhrc.gov/pavement/pccp/petro.

3.1 Sample Receiving and Preparation

Sixteen 6-in diameter cores from bridge barriers at eight different locations in Michigan were provided to Michigan Tech by WSU. These barriers were constructed between 1983 and 2001. Specifics regarding the precise locations of these barriers are provided in the next chapter. Upon receipt, the cores were cataloged and inspected visually in order to assess the general conditions of the concrete and to detect possible diagnostic features. After completion of the visual inspection, specimens were prepared for petrographic examination.

First, the more friable or broken up cores were glued back together using an epoxy resin. Then two slabs, approximately 25-mm thick, were sliced lengthwise from each core (perpendicular to the finished surface), using a kerosene cooled diamond-bladed rotary saw. After at least one night in a thermostated drying cabinet at temperatures not exceeding 60°C, one slab was prepared for air-void examination and optical microscopy, and the other slab was used to determine the carbonation depth and to make thin-sections.

The slab prepared for air-void analysis was ground on one side with progressively finer abrasives (200 through 500-grit paper) on a rotating lap. The final polishing was done with 600-grit silicon carbide in order to provide a planar and smooth surface where the air voids and the aggregates could be clearly distinguished from the cement paste.

The slab used for thin sections was sectioned into billets of approximately 3.5 cm x 4 cm using a rotary saw with a thin, smooth edged diamond blade running in a kerosene bath (oil-based

lubricants do not dissolve reaction products and secondary minerals as readily as water-based lubricants). From each slab, at least two billets were made into thin-sections, one from the top (surface of the bridge barrier) and one from the bottom portion of the slab. The production of the thin sections can be summarized as following:

1. Glue the billet on a 46 mm x 27 mm glass slide
2. Reduce the thickness of the billet to 10.5 mm (including the thickness of the glass slide) using a diamond edged cutoff saw with a very thin blade.
3. Progressively grind the surface of the billet using an automatic section grinder (Dansk Beton, Model DBT diamond roller grinder), cooled with propylene glycol, to a thickness of 10.12 mm including glass slide (the thickness is measured using a micrometer screw gauge)
4. Clean the billets for 5 min in a sonic bath with 200 proof ethyl alcohol as cleaning medium.
5. Wipe off the prepared face of the billet and vacuum impregnate it with fluorescent epoxy (1 percent).
6. Grind the impregnated surface to remove the excess epoxy including 0.007 mm of the surface of the work piece.
7. Clean the billets with acetone.
8. Bond the plane ground surface of the billet to a 7.5 cm x 5.0 cm microscope slide using mounting epoxy.
9. Cut the billet from the smallest glass slide, leaving at least a 0.2 mm thick layer of specimen on the microscope slide.
10. Grind the thin section to a final thickness of 0.03 mm at very slow speed in order to prevent scattering (control the thickness based on polarization colors using a thin section viewer).

3.2 Stereo Optical Microscopy

The polished slabs were examined with a stereo-optical microscope at magnifications varying from 10X to 70X. Subsequently, the specimens were stained with a solution of barium chloride and potassium permanganate (2:1 ratio barium chloride to potassium permanganate in a 6 percent water solution). The barium chloride/potassium permanganate (BCPP) stain is used to detect sulfate minerals, such as ettringite, gypsum, and anhydrite phases that might have infilled air voids and cracks by selectively coloring the sulfate minerals purple (Poole 1974). The

solution was spread on the samples with a small glass plate and rinsed off with oxalic acid after 2 min to remove any surface coloration. Once the slabs were dry, the parameters of the air-void system were observed according to the modified point count method described in ASTM C457, using a stereomicroscope with an automated stage and a magnification of 70X.

3.3 X-Ray Analytical Microscopy

Before the impregnation with epoxy (between step 4 and 5 of the thin sectioning procedure), characteristic x-ray maps were recorded using the Oxford XGT x-ray analytical microscope of samples where some signs of ASR had been detected during the inspection with the stereo optical microscope. Those maps were taken under vacuum conditions, with an accelerating voltage of 30 kV, a beam current of 1mA, and an x-ray gun tube of 100 μm resolution. Each map scanned an area of 6.5 mm by 6.5 mm for a total duration of 2 hours, and a resolution of 256 x 256 pixels (25 μm/pixel).

X-ray analytical microscopy is used to obtain compositional information of solid samples by measuring the energy and intensity distribution of the characteristic x-ray signals generated by a focused x-ray beam. The characteristic x-ray signals are produced when an incident x-ray photon ejects an electron from the inner shell of a specimen atom, and the atom fills the inner-shell vacancy with an outer shell electron. Indeed, when the electron goes from the outer shell to the inner shell in order to fill the vacancy, it goes from a higher energy state to a lower energy state; the difference in energy between those two stages is released in the form of a photon. That photon has a well-defined energy that is specific for each element, and for the layers involved. For example, each element produces specific K_α, and K_β x–rays. The K_α x-rays are produced when a vacant spot in the most inner shell (K shell) is filled by an electron from the next shell out (L shell), and the K_β x-rays are produced when a vacant spot in the K shell is filled with an electron from the shell following the next shell out (M shell) (Goldstein 2003).

3.4 Petrographic Optical Microscopy

The fluorescent epoxy impregnated thin sections were viewed in a petrographic microscrope, using three different types of illumination: transmitted plane polarized light, transmitted cross polarized light and epifluorescent illumination at magnifications of 5X, 10X, 20X, and 50X. The

polarized features are useful in the identification of various minerals (aggregates, secondary mineralization, and reaction products) based on different degrees of refraction associated with different materials. On the other hand, the fluorescence mode is essentially used to distinguish empty spaces (cracks in aggregates and paste, porosity of the paste and the aggregates) from colorless substances with zero birefringence. Some cracks are inevitably created during the final thinning process of the section; however, with the fluorescent mode it is possible to determine if the crack was inherent in the specimen since only the later was present at the time of impregnation and is filled with fluorescent dye (FHWA 1997).

3.5 Scanning Electron Microscopy

An environmental scanning electron microscope (ESEM) coupled with an energy dispersive spectrometer (EDS) was used to confirm the results of the stereo and petrographic optical microscope evaluation. The principles of the x-ray qualitative analysis performed with the SEM-EDS or with the x-ray analytical microscope are similar. One difference is that with the SEM-EDS, the atoms of the sample are excited by electrons, while in the x-ray analytical microscope they are excited by rhodium x-rays. Also, the EDS generated x-ray maps were recorded with a higher resolution, and x-ray spectrums were recorded for secondary deposits.

Prior to examination, the thin sections of interest were coated with carbon in order to avoid accumulation of charge (due to electron bombardment) on the surface of the specimens. All the measurements were taken under a high vacuum at an accelerating voltage of 15 keV, working distance of 10 mm, 0 degree tilt, 35 degrees take-off-angle, 50 ms dwell time, and 10 percent dead time. Each map scanned an area of 1.28 mm by 1.00 mm for a total duration of 5.8 hours, and a resolution of 512 x 400 pixels (2.5μm/pixel).

3.6 Determination of the Carbonation Depth

After preparation of the thin sections, one billet from to the outer surface of the bridge barrier remained for each location. Those billets were polished on the rotating lap (like the slabs for air-void analysis) and sprayed with a mixture containing 0.5 percent phenolphthalein in a 50/50 solution of water and isopropyl alcohol. Phenolphthalein changes from colorless to pink over the pH range of 8.3 to 10. Since the pH of the concrete is normally higher than 10, but for fully carbonated paste is around 8.4, the paste turns pink except where it is fully carbonated, allowing the measurement of the carbonation depth.

Chapter 4. Results and Discussion

The results of applying the analytical approach described in "Guidelines for Detection, Analysis, and Treatment of Materials-Related Distress in Concrete Pavements – Volume 2 (Van Dam 2002b)" are summarized in this chapter of the report. Detailed test results for each bridge are provided in project portfolios in Appendix A.

4.1 Visual and Stereo Optical Microscope Analysis

The locations of each bridge evaluated and the observations of the cores made during the visual and stereo optical microscope examinations are summarized in table 1. In the observations provided in table 1, figures 1 through

4.2 Air-Void Analysis

The results of the air-void analysis by the modified point count method (ASTM C457) are summarized in table 2. Figure 8 plots the air contents and figure 9 the spacing factors for the cores evaluated. In order to evaluate the original air-void system of the samples, an attempt was made to record the number of filled air voids as well as the number of empty voids (ASTM C457, requires only the computation of the existing air voids, since only they can actually protect the paste against frost damage). Unfortunately, the BCPP staining method employed to selectively stain the ettringite filled voids purple did not provide the desired results, coloring both the paste and the filled voids light pink. This made it very difficult to observe a difference between the two. However, an approximate evaluation of the extent of the filled air voids had been recorded during the examination with the stereo optical microscope that preceded the staining procedure.

Table 1. Summary of core logs for sites included in this study.

Core location/ Bridge ID	Year	WSU ID	MTU ID	Observations
I-75 over 13 Mi Rd S021-63174	2001	5	A1	0.75-inch crushed tan carbonate coarse aggregate (limestone or dolomite). Gap in the gradation of the aggregates in A2 (figure 1). Small entrapped air voids, no rebar in the cores. Some fine cracked siltstones with aggregate-paste bond failure (cracks generally not extending far in the paste) (figure 2).
		8	A2	
I-75 over Clarkston Rd S15-63172	1989	6	B1	Mix of 0.75-inch crushed and natural gravel coarse aggregate. Rebar is present in both cores. A lot of irregularly shaped small entrapped air-voids around the aggregates and rebar (figure 3). No rust on the rebar.
		10	B2	
I-75 over Clintonville S12-63172	1988	6	C1	0.75-inch natural gravel coarse aggregate. Rebar present in C2, no rust, well adhering paste. Some entrapped air voids (figure 3).
		10	C2	
I-75 over Auburn Rd S021-632174	2001	3	D1	0.75 inch crushed tan carbonate coarse aggregate. Bad consolidation around the rebar in D1, no rust. Smaller gaps around some of the aggregates (figure 4).
		4	D2	
I-96 over M43 S02-23152A	1980	1	E1	0.75-inch natural gravel coarse aggregate. Rust on the rebar in both samples, paste does not adhere very well to it. Separation of the layer of concrete right above the corroded rebar in E2 (figure 5).
		5	E2	
I-94 over Merriman S04-82022	1993	6	F1	0.75-inch blast furnace slag coarse aggregate. Big entrapped air void on one side of the rebar in F2, no rust. Some small entrapped air voids in the paste (figure 6). A lot of cracked fine cherts with reaction rims and cracked fine black siltstones, cracks go through the paste (a sign of ASR). Map cracking on the top surface of the cores.
		8	F2	
I-69 over Clark Rd S01-44044	1983	7	G1	0.75-inch crushed tan carbonate coarse aggregate. Very poor consolidation (especially G2), a lot of entrapped air. Core G2 is broken in two pieces (figure 7). No rebar.
		10	G2	
I-94 over Middlebelt S06-82022	1993	2	H1	0.75-inch blast furnace slag coarse aggregate. Some entrapped air-voids (figure 6). Rebar with a little rust on the sides is present only in H1. Several fine black siltstones with lengthwise crack, and cracked cherts with reaction rims, cracks go through the paste (a sign of ASR).
		4	H2	

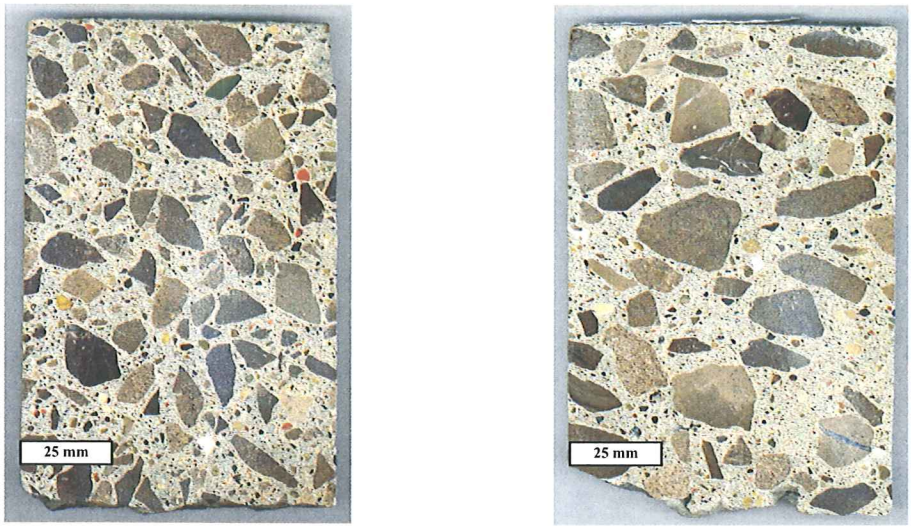

Figure 1. Difference in the gradation of the aggregates from core A1 (left) and A2 (right), polished slabs.

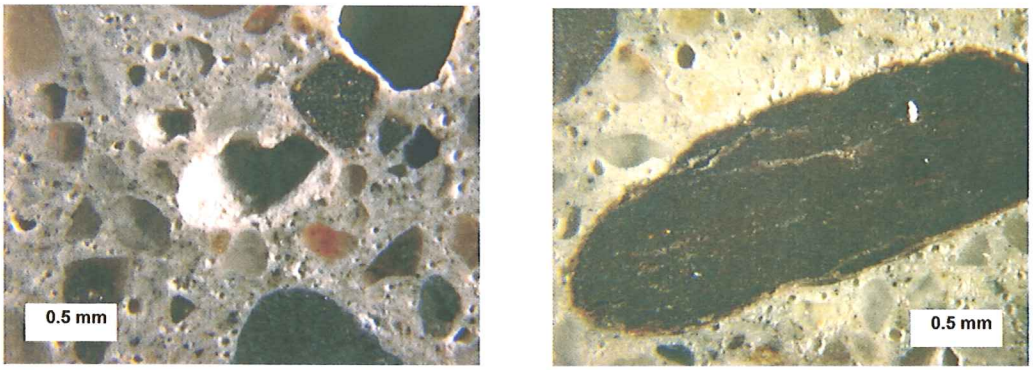

Figure 2. Stereo optical micrograph of typical entrapped air void and cracked siltstone in core A2.

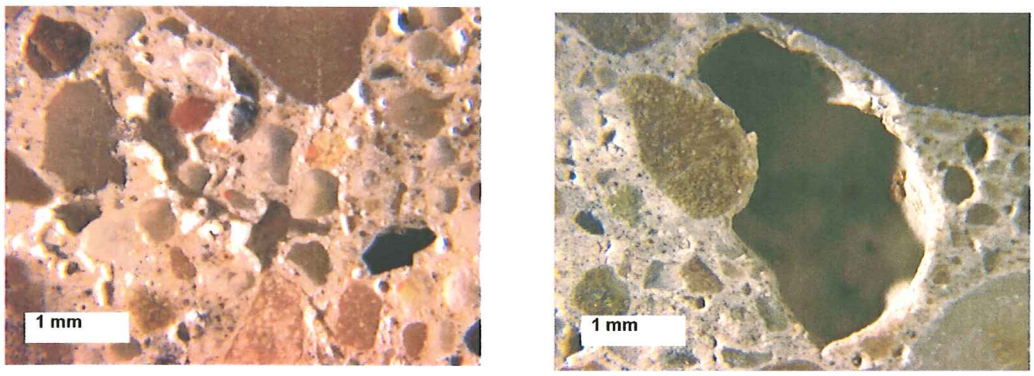

Figure 3. Stereo optical micrographs of entrapped air in specimens B1 (left) and C2 (right).

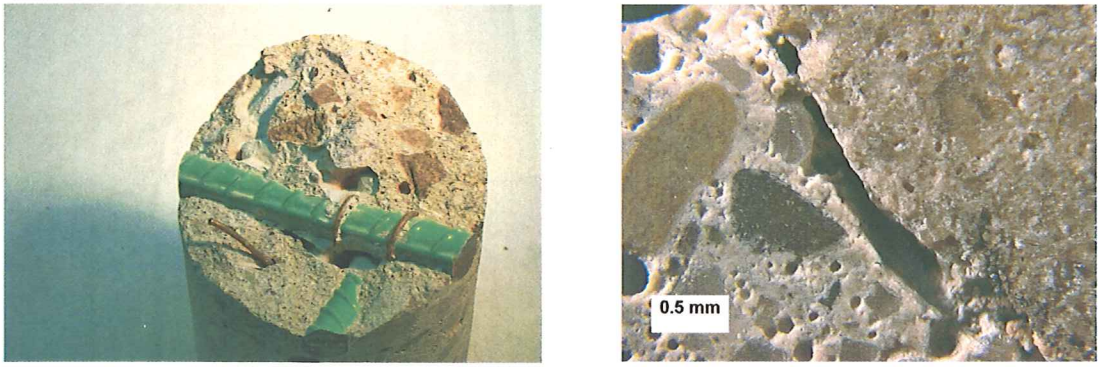

Figure 4. Entrapped air in sample D1, around rebar (left) and aggregate (right).

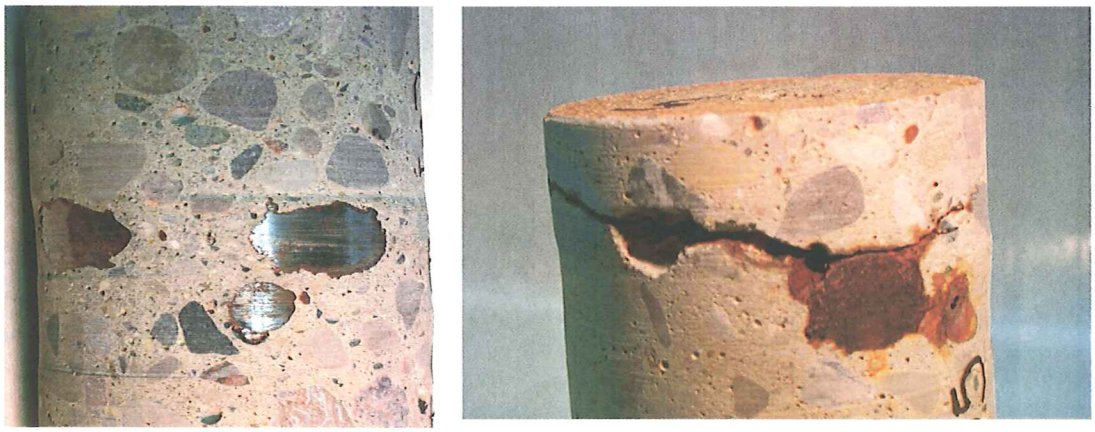

Figure 5. Corrosion of reinforcing steel in cores E1 (left) and E2 (right).

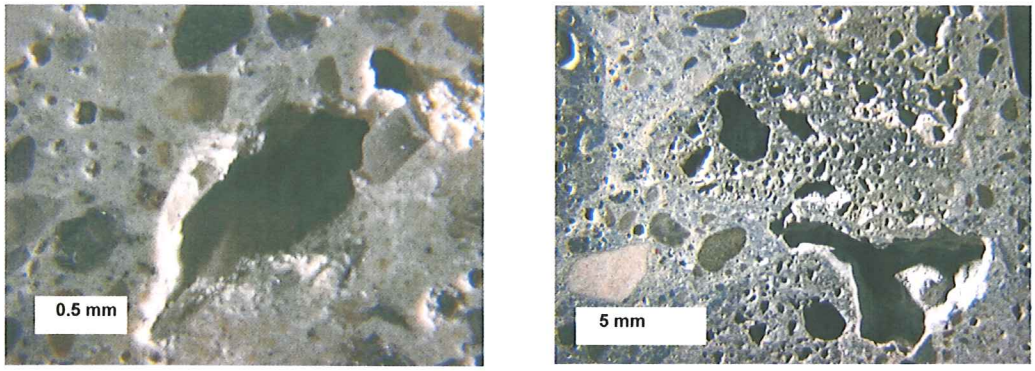

Figure 6. Stereo optical micrographs of entrapped air voids in cores F2 (left) and H1 (right).

Figure 7. Honeycombing in core G2.

As can be seen in table 2 (the highlighting is used to identify samples exceeding recommended limits) and figures 8 and 9, the samples from locations A, B, D, E, all have an adequate spacing factor (< 0.200 mm) and specific surface (> 25mm^2/mm$^{3)}$, and no or little filling of the air void system. Samples from location A and B have an air content slightly under the limit normally specified for concrete with 0.75 in maximum size aggregate (6 percent); however, since the other air-void parameters are within safe limits, the protection against freeze-thaw damage should be adequate. For location A, the low air content is due to the very small size of the air voids, while for location B it results from a lower paste content. Figure 10 shows the air-void systems of A2 and D1. Both samples have similar spacing factors, but the air content of A2 is lower because the air-voids are much smaller than in D1.

Table 2. Summary of the air-void system parameters.

ID MTU	Existing Specific surface (α) mm	Existing Air Content (Area percent)	Existing Spacing Factor (mm)	Paste (Area percent)	Coarse Aggregate (Area percent)	Fine Aggregate (Area percent)	Importance of filled air voids
A1	40.1	5.6	0.112	26.4	37.4	30.6	None
A2	51.0	4.7	0.088	22.0	47.1	26.3	None
B1	36.1	4.2	0.123	19.0	39.1	37.7	Minor
B2	42.6	4.4	0.107	21.0	46.3	28.0	Minor
C1	35.8	6.5	0.072	16.9	50.6	25.9	Minor
C2	23.7	5.0	0.206	28.2	30.3	36.3	Minor
D1	36.2	7.3	0.072	19.1	40.1	33.6	None
D2	31.0	9.3	0.076	21.9	41.0	27.8	None
E1	28.8	7.0	0.120	24.3	42.5	26.2	Minor
E2	30.4	7.7	0.096	22.5	45.7	24.2	Minor
F1	15.4	8.9	0.203	27.4	30.6	32.7	Very Important
F2	25.4	6.6	0.173	29.2	45.6	18.4	Important
G1	9.9	6.0	0.434	25.1	29.8	38.0	Very Important
G2	3.7	7.8	0.784	22.0	39.9	29.2	Very Important
H1	19.1	12.6	0.180	26.1	43.0	20.4	Important
H2	7.656	12.82	0.30452	28.96	28.7	28.6	Very Important

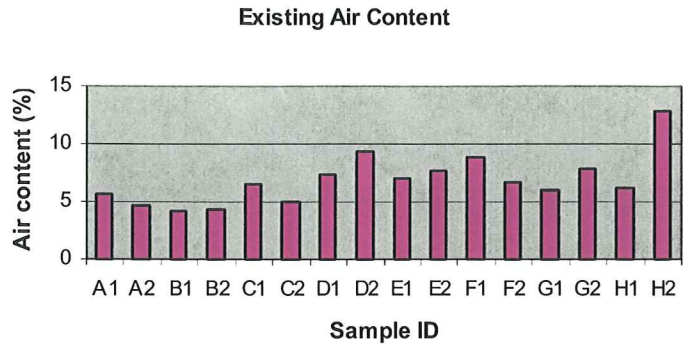

Figure 8. Air content of cores evaluated.

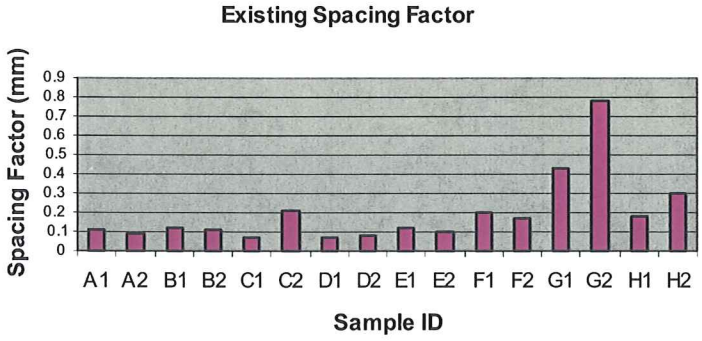

Figure 9. Spacing factor of cores evaluated.

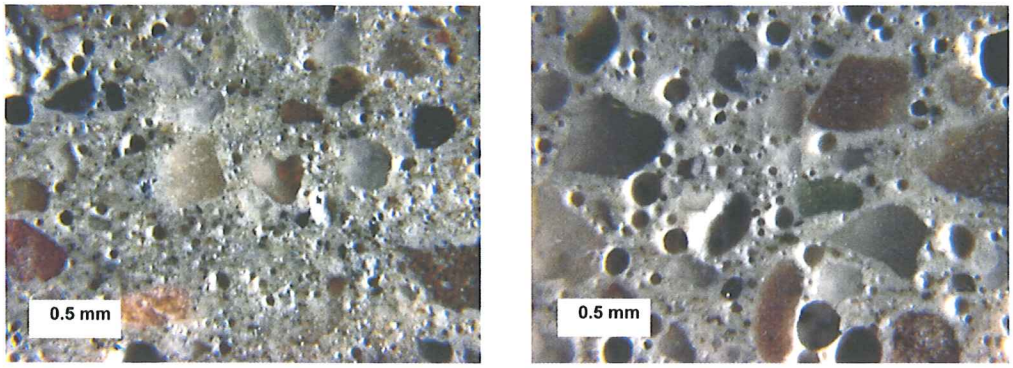

Figure 10. Stereo optical micrograph of air-void structure in A2 (left) and D1 (right).

At locations F and H, the existing air content is well above the specified limit; however, the existing spacing factor is just above or below the limit of 200 μm, depending on the sample. For those two locations, the high spacing factors result from the fact that some air voids are filled with secondary ettringite. Seeing the amount of filled air voids observed, the original air content of these samples was probably grossly over the specified limit and the spacing factor adequate. The two samples from location C show different results, one slab has a spacing factor well below the limit and the other slab has a spacing factor above the limit. Contrary to locations F and H, the high spacing factor in the case of C2 is not due to a large quantity of filled air-voids, but rather to a lack of initial air voids. Figure 11 shows stereo-optical micrographs of the air-void structure in concrete from sites F and C. The white "dots" in concrete from site F are ettringite filled voids.

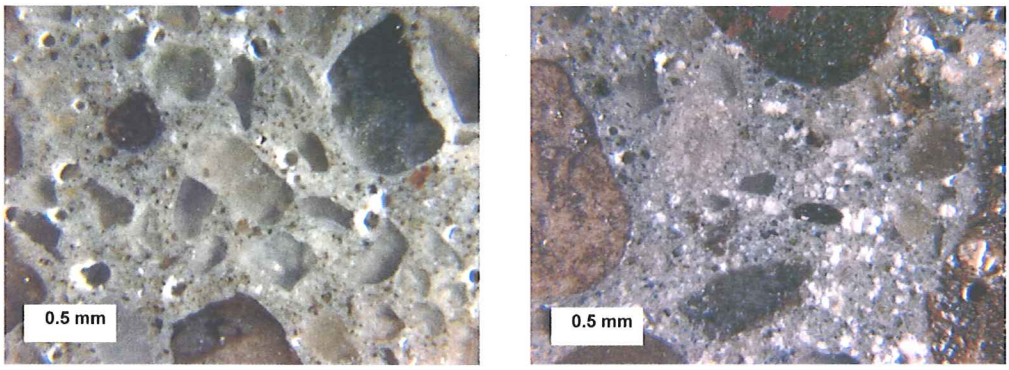

Figure 11. Stereo optical micrographs of air-void structure from C2 (left) and F1 (right).

Samples G1 and G2 are the "worst" with regard to the air-void system. Both samples have high measured air contents only because of the numerous interconnected large entrapped air voids, indicating inadequate consolidation. As can be seen from figure 12, few entrained air voids are present in the concrete and most of them are filled with ettringite (the dissolution and recrystallization of primary ettringite was probably facilitated by poor consolidation), so the existing spacing factor of those slabs is significantly higher than the safe limit, and the barriers are highly susceptible to freeze-thaw deterioration. In these samples, the filled voids were a little easier to distinguish from the paste, so an attempt was made to record the filled air voids during the point count. The original spacing factors (calculated including the filled and empty air voids)

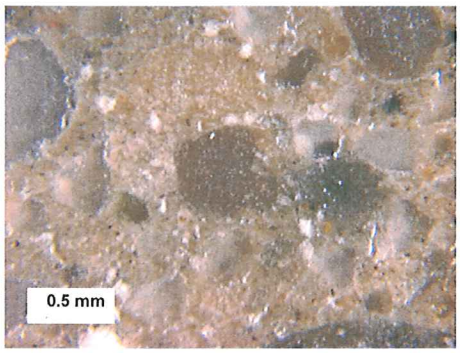

Figure 12. Stereo optical micrograph of air-void system in G2.

were estimated at 0.21 mm and 0.308 mm for G1 and G2, respectively, which are less than half of the existing spacing factors, but still in excess of the 0.2 mm limit. This means that even before the infilling, the amount of air-entrained voids might not have been satisfactory.

4.3 X-Ray Analytical Microscopy

During the inspection with the stereo-optical microscope, signs of alkali-silica reactivity (ASR) were observed in the chert and siltstone fine aggregates of the samples from locations F and H, and some cracked siltstones were noticed in samples from location A. Therefore, several x-ray maps were produced of those samples. Figures 13 and 14 present x-ray maps recorded from samples F2 and H1, respectively. On the left side is the x-ray map presented as an RGB picture, where the red channel is used for the calcium, the green channel for the potassium and the blue channel for the silicon. On the right is a picture of the corresponding location on the sample. Note in figure 13 the high presence of potassium (present in the alkali-silica gel) in the cracks of the fine chert, starting in the aggregate and extending in the paste, and the presence of a cracked black siltstone in the upper right corner.

Figure 14 shows a carbonate aggregate (from H1) containing some inclusions of silicon that seems to be undergoing ASR. Some reacted chert and cracked siltstone can also be observed on the right of the carbonate rock. However, from those maps, and all the other maps that were recorded with the x-ray analytical microscope it is not obvious if the potassium in the siltstones is present as a result of ASR or as a natural constituent of that type of aggregate. This is because it is distributed throughout the aggregates instead of being concentrated in the cracks.

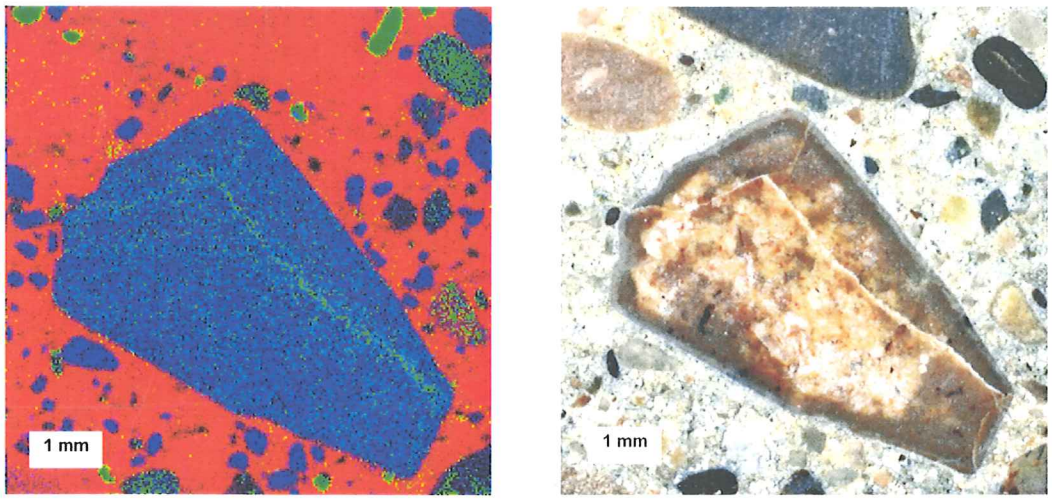

Figure 13. X-ray map (left) and picture (right) of reacted aggregates in specimen F2. Red: Ca, green: K, blue: Si.

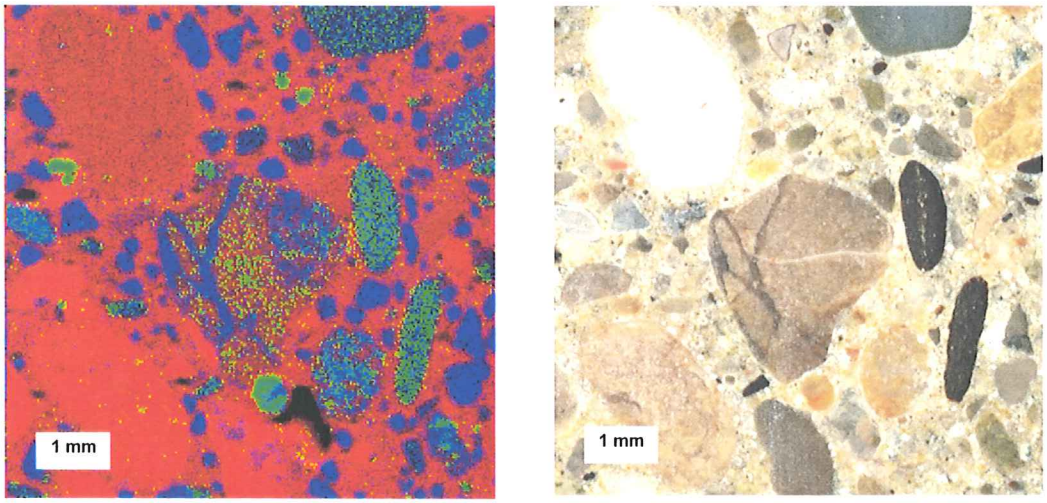

Figure 14. X-ray map (left) and picture (right) of reacted aggregate in core H1. Red: Ca, green: K, blue: Si.

4.4 Petrographic Optical Microscopy

Thin sections confirm the alkali-silica reactivity of the cherts (figure 15), but also of the siltstones in locations F and H (figure 16). Cracks in the fine siltstones from locations F and H clearly extend through the paste, but deposits of alkali-silica gel are more important in location F.

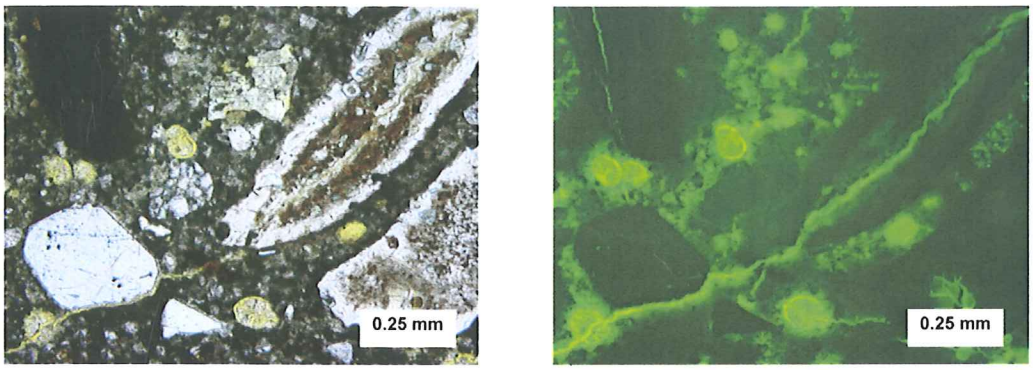

Figure 15. Petrographic micrograph of reacted chert and ettringite filled voids in F1, plane polarized light (left), epifluorescent mode (right).

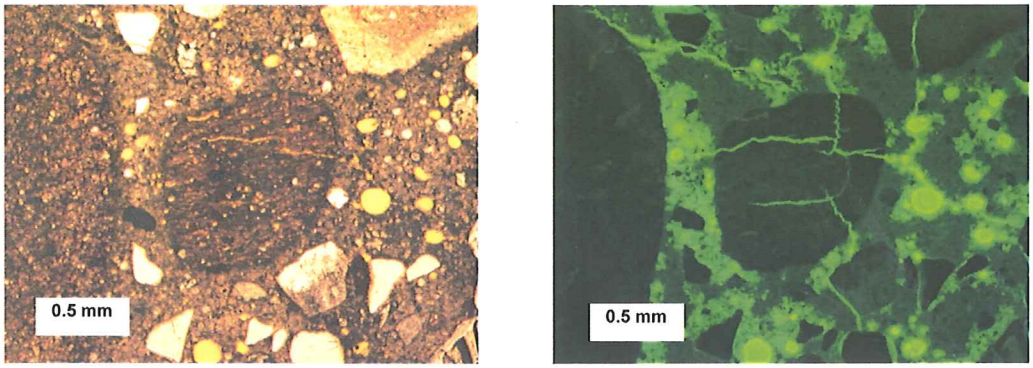

Figure 16. Petrographic micrograph of reacted siltstone in H1, plane polarized light (left), epifluorescent mode (right).

Thin sections from location A, when observed in epifluorescent mode (figure 17), indicate that the cracks in the siltstones do no reach as far from the aggregate, are not as wide open, nor as numerous as for locations F and H. Moreover, no gel was observed in transmitted plane polarized light, so ASR is less probable cause of the cracking unless the reaction is in an early stage. Cracking of the siltstones at location A might be due to freeze-thaw deterioration. Indeed, the siltstone aggregates have a very porous microstructure, and as was also observed in stereo-optical analysis, the boundary between the paste and the fine siltstones was sometimes destroyed, possibly as a result of volume changes or the expulsion of water from the aggregate during freezing and thawing. In the case of locations F and H, the deterioration by ASR linked to the siltstones might also have been aggravated by frost action.

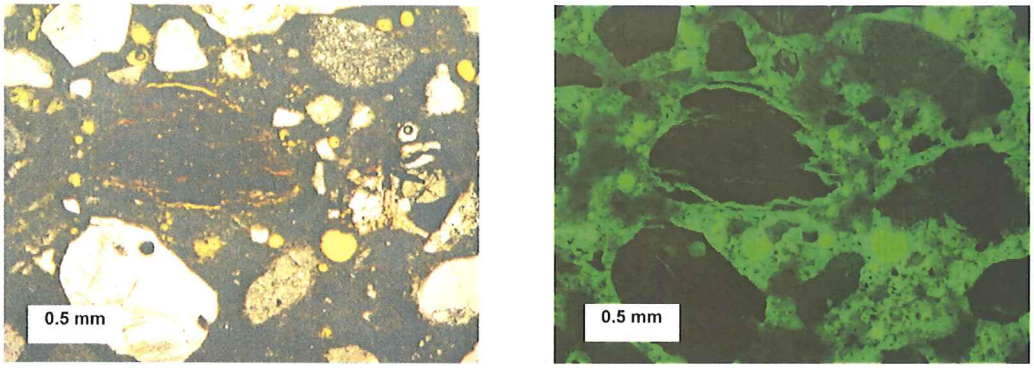

Figure 17. Petrographic micrograph of siltstone in A1, transmitted plane polarized light (left) and epifluorescent mode (right).

Finally, ettringite was observed infilling air voids in thin sections from locations F, G and H. The infilling was particularly important at locations F and G. Figure 18 shows a typical air void filled with needle-like crystals of ettringite from core G2.

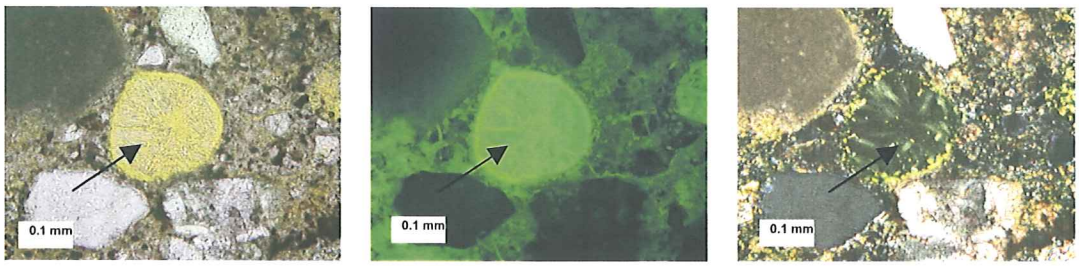

Figure 18. Petrographic micrograph of ettringite filled air void in G2, from left to right plane polarized light, epifluorescent mode and cross polarized light.

4.5 Scanning Electron Microscope Tests

The SEM-EDS was used to supplement the results of the stereo and petrographic optical microscopy. X-ray spectra and x-ray maps confirmed the identity of alkali-silica gel in the cracked siltstones at location F, and of ettringite in air voids from locations F, G and H. No alkali-silica gel was found in the siltstones from location A. Figure 19 shows an SEM image (in backscattered mode) of a cracked siltstone from location F with gel filling the crack and an adjacent air void (indicated with an arrow on the image), and an x-ray spectrum recorded at the location of the infilling, confirming the identity of alkali-silica gel. Figure 20 presents an SEM

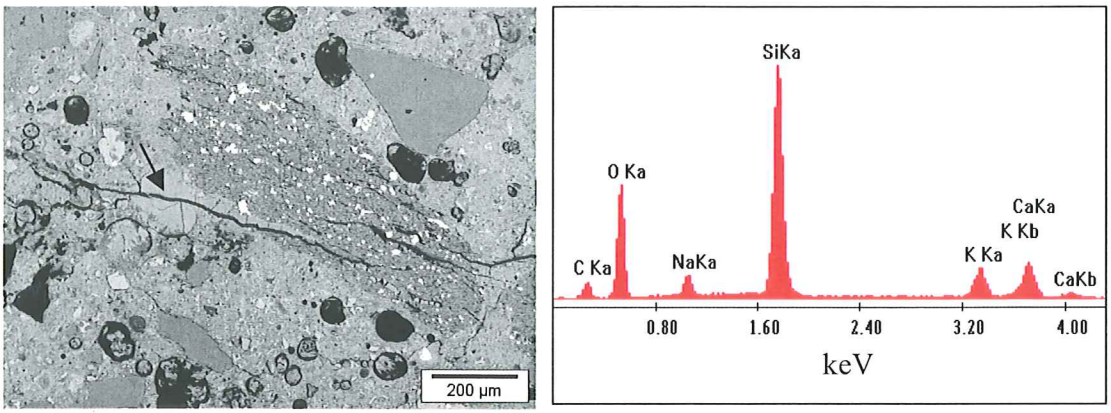

Figure 19. SEM image and x-ray spectra of ASR gel deposit from a reactive siltstone in F1.

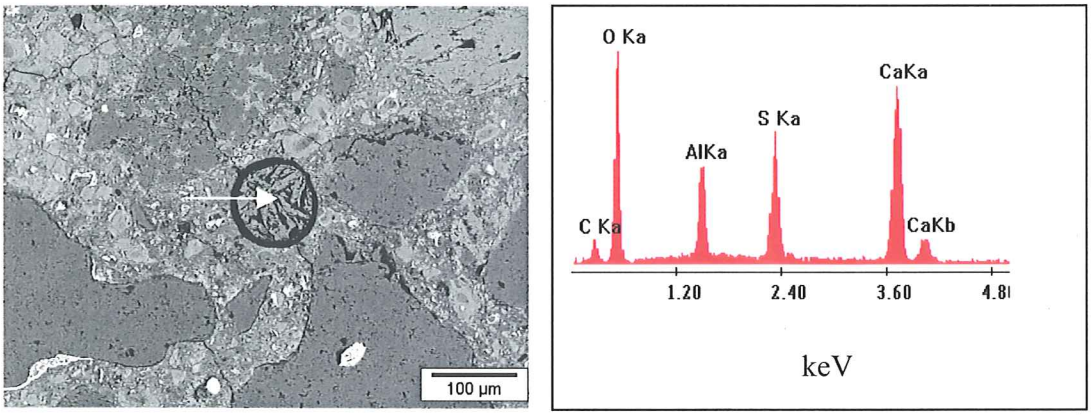

Figure 20. SEM image and x-ray spectra of ettringite infilling air void in G2.

image of a filled air void in G2 with the corresponding x-ray spectrum, confirming the presence of ettringite (calcium sulfoaluminate).

4.6 Carbonation

The depths of carbonation measured from the samples stained with a phenolphthalein solution are summarized in table 3. Where the depth of carbonation was not uniform, which was usually the case, the deepest and shallowest measurements are given.

Table 3. Depth of carbonation.

Sample ID	Depth of Carbonation (mm)
A1	1-3
A2	1-2
B1	2-5
B2	2-4
C1	2-4
C2	1-3
D1	1
D2	2
E1	4-10
E2	1.5-4
F1	0.5-4
F2	1-3
G1	2-4
G2	1.5-3
H1	2
H2	1-3

In general, the average depth of carbonation was relatively small for all the observed samples, indicating that the outer layer of the concrete does not seem to be abnormally porous. However, samples B, E, and G have an average carbonation depth greater than 2 mm, which might indicate a concrete of lesser quality (density). In samples E and F the depth of carbonation varies greatly, indicating the presence of preferential pathways (e.g. cracks). Part of a phenolphalein stained polished billet from site F is shown in figure 21, the pink color corresponds to the uncarbonated paste. The great variation of the carbonation depth in concrete F might be related to map cracking present at the surface of the concrete as a result of ASR.

4.7 Summary

Most of the cores examined show at least some consolidation problems; however, size and quantity of entrapped air voids vary greatly among the samples, going from small voids in samples from location A to honeycombing in specimens from location G. The air-void systems of samples A, B, and D are adequate, although the air contents of cores from locations A and B are a little lower than normal. For locations C, F, and H the spacing factor is not adequate.

Figure 21. Part of phenolphtalein stained polished slab from F1, showing variation of carbonation along the surface.

In the case of locations F and H, a lot of entrained air voids are present, but most of them are filled, whereas for location C there seem to be a lack of entrained air voids but not much infilling. The cores from location G also have an inadequate spacing factor, due to extensive ettringite infilling of existing air-voids and possibly lack of initial air voids. The barriers at that location are thus susceptible to frost damage.

Evidence of alkali-silica reaction was apparent in several of the fine aggregate particles (cherts and siltstones) of the samples containing slag coarse aggregates (F and H). The reaction is manifest as internal cracking of the fine aggregate particles, often extending out into the surrounding cement paste, and by the presence of alkali-silica gel. The reactive siltstones were also observed to be very porous, and might thus be frost-susceptible in addition to being reactive. The extensive presence of ettringite in the air voids of those samples was probably favored by the increased permeability resulting from the deterioration by ASR.

The siltstones that were observed to be reactive at locations F and H were also observed at location A, but in the case of location A, no gel was present and the cracks did not extend appreciably into the paste. It is thus less probable that the siltstones at location A are undergoing ASR; however, the observed cracks might be a result of freeze-thaw deterioration. The fact that the siltstones at location A are not as cracked in the same manner as in those from locations F and H might be due to the absence of reactive cherts, different environmental conditions,

different mix designs, or simply to the fact that the bridge barriers from location A are relatively young (ASR might be in an early stage), and that the fraction of siltstones in the fine aggregate is smaller than for F and H.

The depth of carbonation of samples from locations B, G and E is a little higher than normal, indicating that these samples might be more permeable to water and aggressive agents (e.g. deicer salts) and more susceptible to corrosion. Corrosion was observed in both samples from location E; in sample E2 it was so severe that it even caused delamination of the concrete at the top of the outermost layer of reinforcing steel.

Chapter 5. Conclusions and Recommendations

In order to identify possible factors contributing to the early deterioration of the current generation of barriers used by MDOT, sixteen cores evaluated from bridge barriers from eight different locations in Michigan. The samples were subjected to a full petrographic evaluation, including stereo and petrographic optical microscopy, x-ray analytical microscopy, and scanning electron microscopy. Based on the results of this investigation, the following conclusions can be drawn:

- All the cores evaluated showed some kind of consolidation problems. Entrapped air voids from varying sizes were common around aggregates and the steel reinforcement. Based on these observations, better consolidation of the concrete barriers is required, as this will minimize the ubiquitous entrapped air that was observed at all locations. This entrapped air reduces the strength of the concrete as well as provides a ready pathways for the ingress of water and aggressive chemical agents (e.g. deicers), reducing the life of the barriers.

- Although no low existing air contents were measured (using ASTM C 457), one third of the samples had air-void spacing factors that are considered marginal for protecting the paste from freeze-thaw damage. These high spacing factors were attributed to a lack of entrained air voids (S12-63172), an extensive amount of infilling (S04-82022, S06-82022), or a combination of the two (S01-44044). It is recommended that the air-void system parameters be verified for the specific job mix formula being used. It is well known that the ability of a given air-entraining agent to create an adequate air-void system is affected by the cement and other admixtures used, and time of mixing. This problem is especially acute in stiff mixtures such as used for slip form paving. Controlling the total volume of air by measure the air content of the fresh concrete is not sufficient to ensure freeze-thaw durability. A more rigorous approach to the assessment of the air-void system parameters of the concrete has the potential to significantly enhance the freeze-thaw durability of these concrete barriers.

- Secondary deposits of ettringite were observed in the air voids of several of the cores evaluated in this study. It would be useful to determine the sulfate content of the samples to

evaluate if there is any relationship between sulfate content and amount of infilling. The determination of the sulfate content would be particularly interesting in the case of the concrete with slag coarse aggregate, because based on previous research conducted at Michigan Tech, the dissolution of calcium sulfide from blast furnace slag aggregates may provide an internal source of sulfate possibly promoting the formation of secondary ettringite (Peterson 1999, Hammerling 1999, Hammerling 2000).

- Alkali-silica reactivity (ASR) was observed in the natural fine aggregate fraction at the two locations where blast furnace slag coarse aggregate was used (S04-82022 and S06-82022). It is recommended that a study be initiated to evaluate the nature of the relationship between ASR in the chert and siltstones constituents of the fine aggregates and the slag coarse aggregate in the concrete. This study would need to consider a broad range of factors including the alkali content of the cement, the impact of supplementary cementitious materials, and the type and volume of reactive constituents in the fine aggregate.

- Siltstones observed in concrete from site S041-63174 were similar to those undergoing ASR, but were not reactive. But limited damage was observed that is attributable to freeze-thaw deterioration. The frost-susceptibility of the siltstones, as well as the presence of secondary ettringite in air voids, might also have exacerbated the distress caused by ASR in locations S04-82022 and S06-82022. Tests should be conducted to evaluate the frost-susceptibility of the deteriorated fine siltstones observed at some locations to determine its contribution, if any, to the observed deterioration.

- Finally, significant steel corrosion was observed for only one test site (S02-23152). In that case the corrosion was so severe that delamination had occurred. The carbonation depth measured in samples obtained from this location were higher than normal, indicating that the corrosion might result from a higher permeability to water and aggressive agents (e.g. deicers). Abnormally high permeability could be the result of poor consolidation or the use of a high water-to-cement ratio mixture.

Chapter 6. References

ACI (1998), *State-of-the-Art report on Alkali-Aggregate Reactivity*, ACI 221.1R-98, 31p.

ASTM C 457-90, Standard Test Method for Microscopical Determination of Parameters of the Air-Void System in Hardened Concrete.

Collins, J. and P. D. Bareham (1986), "Alkali-Silica Reaction: Suppression of Expansion Using Porous Aggregate", *Cement and Concrete Research*, vol. 17, Pergamon Journals, LTD., pp. 89-96.

Detwiler, R. J., and L. J. Powers-Couche (1999), "Effect of sulfates in concrete on their resistance to freezing and thawing", *Ettringite the Sometimes Host of Destruction*, Farmington Hills, MI, ACI SP 177-12, Bernard Erlin, pp.219-247.

DePuy, G.W. (1994), "Chemical Resistance of Concrete", *Significance of Tests and Properties of Concrete and Concrete Making Materials,* American Society for Testing and Materials, STP 196C, Philadelphia, PA. pp. 263-281.

Dobie, T.R. (1986), "Correlation Water-soluble alkalies to Total Alkalies in Cement-Considerations for Preventing Alkali-silica Popouts on Slabs", *Alkalies in Concrete*, ASTM STP 930, V.H. Dodson, ED., American society for testing and materials, pp. 46-57.

Fagerlund, G. (1997), "On the service life of concrete exposed to frost action", *Freeze-Thaw durability of Concrete*, E&FN Spon. ISBN: 0-419-20000-2, pp. 23-39.

Famy, C., and H.F.W. Taylor (2001), "Ettringite in Hydration of Portland cement Concrete and its Occurrence in Mature Concretes", ACI Materials Journal, vol. 98, no. 4, pp. 350-356.

FHWA (1997), *Petrographic Methods of Examining Hardened Concrete: a Petrographic Manual*, US Department of Transportation, Federal Highway Administration, FHWA-RD 97-146.

Fournier, B., M. Berubé, and C.A. Rogers (1999), "Proposed Guidelines for the Prevention of Alkali-Silica Reaction in New Concrete Structures", *Transportation Research Record 1668: Concrete in Pavements and Structures*, Transportation Research Board, Washington, D.C, pp. 48-59.

Goldstein, J., D. Newburry, D. Joy, C. Lyman, P. Echlin, E. Lifshin, L. Sawyer, and J. Michael (2003), *Scanning Electron Microscopy and X-ray Microanalysis,* Kluwer Academic/ Plenum publishers, New York, p. 689.

Guédon, J.S., and A. Le Roux (1994), "Influence of Microcracking on the Onset and Development of the Alkali Silica Reaction", *Durability of concrete*, Third International Conference, Nice, France, ACI SP-145, V.M. Malhotra, pp. 713-720.

Hammerling, D.M. (1999), "Calcium sulfide in Blast Furnace Slag used as Concrete Aggregate", Thesis for the Degree of M.S., Michigan Technological University, p. 70.

Hammerling, D.M., K.W. Peterson, L.L.Sutter, T. J. Van Dam, and G. R. Dewey (2000), "Ettringite: not just in Concrete", *Proceedings of the 22nd International Conference on Cement Microscopy*, Montreal, Canada.

Hazrati, K., C. Abesque, and M.Pigeon (1997), "Efficiency of Sealers on the Scaling Resistance of Concrete in Presence of Deicing Salts", *Freeze-Thaw durability of Concrete*, E&FN Spon., pp.165-196.

Helmuth, R., and D. Stark (1992), "Alkali-Silica Reactivity Mechanisms", The American ceramic society, Westerville, OH. ISBN 0-944904-55-6, pp. 131-208.

Ho, D.W.S, and R. K. Lewis (1987), "Carbonation of Concrete and its Prediction", *Cement and concrete research*, Vol 17, pp. 489-504.

Hunt, D.M., and L. A. Tomes (1962), "Reaction of Hardened Portland Cement Paste with Carbon Dioxide", *Journal of Research of the National Bureau of Standards-A, Physics and Chemistry*, Vol. 66A, no 6, pp. 473-481.

Jacobsen, S, and E.J. Sellevold (1997), "Frost/salt Scaling and Ice Formation of Concrete: Effect of Curing Temperature and Silica Fume on Normal and High Strength Concrete", *Freeze-Thaw durability of Concrete,* E&FN Spon. ISBN: 0-419-20000-2, pp. 93-105.

Johansen, V, N. J. Thaulow, and J. Skalny(1993), "Simultaneous Presence of Alkali-Silica Gel and Ettringite in Concrete", *Advances in Cement Research*, vol. 5, no17. pp. 23-29.

Johnston, C.D. (1994), "W/cm Code Requirements Inappropriate for Resistance to Deicer Salt Scaling, *Durability of concrete.* Third International Conference, Nice, France, ACI SP-145, V.M. Malhotra, pp. 85-93.

Krogh, H. (1975), "Reaction of Silica and Alkalies", Symposium on Alkali-Aggregate Reaction Preventive Measures, Reykjavik, august 1975, pp. 132-159.

Lane, D.S. (1992), "Alkali-Silica Reactivity: An Overview of a Concrete Durability Problem", *Materials, Performance and Prevention of Deficiencies and Failures*, Proceedings of the Materials Engineering Congress, Atlanta, GA., American Society of Civil Engineers, New York, pp. 231-244.

Litvan, G.G. (1978), "Freeze-thaw durability of porous materials", *Durability of building materials and components: proceedings of the first international conference,* ASTM special technical publications 691, pp. 455-463.

Marchand, J., EJ. Sellevold, and M.Pigeon (1994), "The deicer salt scaling deterioration of concrete – An overview", *Concrete Durability,* Third International Conference, Nice, France, ACI SP-145, V.M. Malhotra, pp. 1-25.

Mindess, J., F. Young, and D. Darwin (2003), *Concrete*, Prentice Hall, Pearson Education, Inc., Upper Saddle River, NJ 07458, 644p.

Ouyang, C and O. J. Lane (1999), " Effect of Infilling Air Voids by Ettringite on Resistance of Concretes to Freezing and Thawing", *Ettringite the Sometimes Host of Destruction*, Farmington Hills, MI, ACI SP 177-12, Bernard Erlin, pp. 249-261.

Petereson K.W., D. Hammerling, L.L. Sutter, T. J. Van Dam, and G.R. Dewey (1999), "Oldhamite: not just in Meteorites", *Proceedings of the 21st International Conference on Cement Microscopy*, Las Vegas, NV, April 25-29.

Peterson, K. (2001), *Air void analysis of hardened concrete via flatbed scanner*, Thesis for the degree of Master of Science, Michigan Technological University, 39p.

Pigeon, M., and R. Plateau (1995), "Durability of Concrete in Cold Climates", E&FN Spon, 244p.

Pleau, R. (1992), La caractérisation du réseau de bulles d'air dans le béton durci comme outil d'évaluation de la durabilité au gel du béton, PhD Thesis, Laval University, Québec.

Poole, A.B., and A. Thomas (1974), "A Staining Technique for the Identification of Sulphates in Aggregates and Concrete", *Mineralogical magazine*, September 1975, vol. 40, pp. 315-16.

Rösli, A., and A.B. Harnik (1980), "Improving the Durability of Concrete to Freezing and Deicing Salts", *Durability of Building Materials and Components*, ASTM STP 691, P.J. Serada and G.G. Litvan , EDS. , American Society for testing and Materials, pp. 464-473.

Scrivener, K.L. (1996), "Delayed ettringite formation and concrete railroad ties", *Proceedings of the 18th International Conference on Cement Microscopy.*

Shoya, M. (1997), "Freezing and Thawing Resistance of Concrete with Excessive Bleeding and its Improvement", *Durability of concrete*, Proceedings Fourth CANMET/ACI International Conference, Sydney, Australia, Volume 2, ACI SP-170, V.M. Malhotra, pp. 879-887.

Staton, J.F. and Knauff, J. (1999), "Performance Evaluation of Michigan's Concrete Barriers," Draft Report, Materials Research Group, Construction and Technology Division, Michigan Department of Transportation, Lansing, MI. January.

Stark, J.,and K. Bollmann (1999), "Laboratory and Field Examination of Ettringite Formation in Pavement Concrete", *Ettringite the Sometimes Host of Destruction*, Farmington Hills, MI, ACI SP 177-12, Bernard Erlin, pp. 183-191.

Stark, J., and J.M. Ludwig (1997), "Influence of Water Quality on the Frost Resistance of Concrete", *Freeze-Thaw durability of Concrete,* E&FN Spon, pp.157-164.

St John, D. A., A W. Poole, and I. Sims (1998), *Concrete Petrography, a Handbook of Investigative Techniques*, Arnold, 474p.

Sutter, L. L. (2001), *An approach to Characterize Materials Related Distress in Portland Cement Concrete Pavements*, Dissertation for the Degree of Ph. D., Michigan Technological University, 294p.

Van Dam, T. J., L.L. Sutter, K.D. Smith, M.J. Wade, and K.R. Peterson (2002a), *Guidelines for the Detection, Analysis, and Treatment of Materials-Related Distress in Concrete Pavements - Volume 1: Final Report, FHWA-RD-01-164*, Federal Highway Administration, McLean, VA.

Van Dam, T. J., L.L. Sutter, K.D. Smith, M.J. Wade, and K.R. Peterson (2002b), *Guidelines for the Detection, Analysis, and Treatment of Materials-Related Distress in Concrete Pavements -*

Volume 2: Laboratory testing, Data Analysis, and Interpretation Procedure for Distressed Concrete Pavements, *FHWA-RD-01-164,* Federal Highway Administration, McLean, VA.

Ymashita, H., K. Sakai, and T. Kita (1997). "Effect of Pore Structure in Concrete on Frost Resistance", *Durability of Concrete*, Proceedings Fourth CANMET/ACI International Conference, Sydney, Australia, Volume 2, ACI SP-170, V.M. Malhotra, pp. 919-925.